Tutors

Dra. Irene García Cano
Departament de Ciència dels Materials i Química Física

Sr. Manuel Alcaine Santamaría
Sedal

UNIVERSITAT DE BARCELONA

Grau d'Enginyeria de Materials

Treball Final de Grau

Selection of thermoplastic materials for application in mixer cartridges based on the tribological properties between polymeric pairs.

Selecció de materials termoplàstics per a aplicació en monocomandaments en base al comportament tribològic entre parells de polímers.

David Sabaté Rovira

June 2018

UNIVERSITAT DE BARCELONA

Dos campus d'excel·lència internacional
B:KC Barcelona Knowledge Campus
HUB Health Universitat de Barcelona Campus

La gemma no pot ser polida sense fricció, així com ningú pot perfeccionar-se sense obstacles.

Confuci

Primer de tot, voldria agrair als meus tutors el Sr. Manuel Alcaine i la Dra. Irene García per l'oportunitat brindada i la confiança, així com a Sedal i al Centre de Projecció Tèrmica per dotar-me dels mitjans necessaris per dur a terme el treball.

Moltes gràcies a tots els companys i companyes de Sedal pels coneixements, les hores dedicades i la bona acollida, i una forta abraçada a l'Aina Cabrer, la Nuria Salazar i al Dr. Vicente Albaladejo pels consells i l'interès mostrat.

Un especial agraïment a la Dra. Ana Inés Fernández per aconsellar-me i guiar-me acadèmica i personalment, i a la Dra. Mercè Segarra per l'atenció i l'ajuda.

Finalment, agrair el suport rebut per part dels meus amics i familiars, i un sincer petó a la Lídia Ocaña per la paciència i l'estima.

Moltes gràcies a tots!

REPORT

CONTENTS

1. GLOSSARY 3
2. SUMMARY 5
3. RESUM 7
4. PREFACE 9
4.1. Project origin 9
4.2. Project scope 10
5. INTRODUCTION 11
5.1. Mixer cartridges 12
5.2. Objectives 15
6. CANDIDATES SELECTION PROCESS 17
6.1. Selection procedure 17
6.2. Housing 18
6.2.1. Contour conditions 18
6.2.2. Creep resistance 19
6.2.3. Mechanical demand 21
6.3. Racord 24
6.3.1. Mechanical tests 29
6.3.2. Dimensional stability 30
6.3.2.1. Dimensional increase associated to moisture absorption 30
6.3.2.2. Thermal expansion 32
6.4. Ceramic Holder 33
7. TRIBOLOGICAL RESEARCH 35
7.1. Experimental equipment 35
7.2. Adaptation of the equipment 36
7.3. Experimental process 40

8. RESULTS AND DISCUSSION 43
8.1. Tribology against POM 43
8.2. Tribology against PBT+15%GF 46
8.3. Tribology against PPE/PS+20%GF 49
8.4. Combination's choice 52
8.4.1. Scores considering a PBT+15%GF based housing 54
8.4.2. Scores considering a PPE/PS+20%GF based housing 56
9. CONCLUSIONS 59
10. REFERENCES AND NOTES 61
APPENDICES 63
Appendix 1: Formulations of the candidates 65
Appendix 2: Sauna conditions simulation test 67
Appendix 3: Endura SN-35 S/D EVO1 drawing 69
Appendix 4: Tribology against POM 71
Appendix 5: Tribology against PBT+15%GF 73
Appendix 6: Tribology against PPE/PS+20%GF 75
Appendix 7: Figures list 77
Appendix 8: Tables list 81

1. GLOSSARY

Polyoxymethylene	**POM**
Polyamide	**PA**
Molybdenum disulfide	**MoS_2**
Glass fibre	**GF**
Polybutylene terephthalate	**PBT**
Polyphenylene ether	**PPE**
Polystyrene	**PS**
Polysulfone	**PSU**
Polyethylene terephthalate	**PET**
Polytrimethylene hexamethylene terephthalamide	**PA6-3-T**
Polyphenylene sulfide	**PPS**
Polyphthalamide	**PPA**
Finite element analysis	**FEA**

2. SUMMARY

The performance of the mixer cartridges that regulates the temperature and the water flow in most of the daily use faucets is based on the movement and geometry of two ceramic discs, whose relative position is set by moving the handle. During the transmission of the movement to the discs, we also submit relative movement to three thermoplastic pieces called ceramic holder, racord and housing, which are in permanent contact and compressed. The tribological behaviour of this system is crucial for the cartridge's performance. Even if different greases are used as lubricants between the pieces, the raw material of these polymers is fundamental in terms of the generated friction and wear.

In the present project, a selection process aimed at enhancing the thermoplastic combination currently used for the components has been done. A first selection phase, in where parameters such as dimensional stability associated to moisture absorption, thermal expansion, mechanical properties, availability or cost have been studied, has been done in order to choose potential substitutes. In a second selection phase, using a ball-on-disk device, tribological tests have been done to those combinations worthwhile to the project.

In the final count, the results show that the current combination can be improved; being the use of polyoxymethylene (POM) in the ceramic holder, polyphthalamide (PPA) filled with 40% glass fibre in the racord and polybutylene terephthalate (PBT) filled with 15% glass fibre in the housing the best combination among those studied.

Key words: Tribology between polymeric pairs, Technical thermoplastics, Friction, Wear, Ball-on-disk, Materials selection, Sedal, Mixer cartridges.

3. RESUM

El funcionament dels monocomandaments que regulen la temperatura i el pas de l'aigua en la gran majoria d'aixetes d'ús quotidià es basa en el moviment i geometria de dos discs ceràmics, la posició relativa dels quals definim en moure el mànec. En el procés de transmissió del moviment als discs, sotmetem també a moviment relatiu tres peces termoplàstiques anomenades tapeta, ràcord i carcassa, que es troben en contacte permanent i comprimits. El bon funcionament tribològic d'aquest sistema és crucial pel bon funcionament del cartutx. Tot i l'ús de grasses com a medi lubrificant entre les peces, la naturalesa d'aquests polímers és bàsica pel que fa a la fricció i abrasió que es genera.

En el present treball s'ha realitzat un procés de selecció enfocat a millorar la combinació de termoplàstics usats actualment en les peces. Una primera fase de selecció en què s'han avaluat paràmetres tals com estabilitat dimensional enfront l'absorció d'humitat, expansió tèrmica, propietats mecàniques, disponibilitat o cost s'ha dut a terme per tal d'escollir els potencials substituts. En una segona fase de selecció, usant un dispositiu *ball-on-disk*, s'han realitzat assaigs tribològics de totes les combinacions interessants pel desenvolupament del projecte.

En el còmput final, els resultats mostren que existeixen millors combinacions que l'actual; sent l'ús del polioximetilè (POM) en la tapeta, la poliftalamida (PPA) amb 40% de fibra de vidre en el ràcord i el polibutilè tereftalat (PBT) amb un 15% de fibra de vidre en la carcassa la millor de les estudiades.

Paraules clau: Tribologia entre parells de polímers, Termoplàstics tècnics, Fricció, Abrasió, Ball-on-disk, Selecció de materials, Sedal, Cartutx monocomandament.

4. PREFACE

4.1. PROJECT ORIGIN

SEDAL is a leading global manufacturer of components for the faucet and sanitary industry. For many years, their mixer cartridges have been using polyoxymethylene (POM) (***65***) both in the racord and in the ceramic holder. POM is a commonly used material in many tribological applications due to its low friction coefficient and high stability [1], but its tribological behaviour become worse when POM performs against itself [2]. There is few information concerning the friction and wear of polymer-polymer combinations, but the most accepted explanation is the tribological behaviour between polymers can be attributed to two main mechanisms: adhesion and deformation [3], and using self-mated material combinations can result in higher adhesion forces [4]. That is why POM-POM pair may cause at the user to have a bad feeling when using the faucet already at the first few times. Trying to avoid this issue, polyamide 66 (PA66) with molybdenum disulfide (MoS_2) (***65***) was chosen as the racord's raw material to friction against the POM based ceramic holder. Even so, polyamides tends to sustain an inappropriate dimensional increase because of its high moisture absorption [4]. After internal tests simulating the cartridge performance in daily usage, this behaviour has been verified (see *Figure* **1**). This increase may

become in the failure of the cartridge by blocking if the racord overpass the tolerances and touches the housing neck.

Thus, an upgraded polymeric combination is needed to improve the cartridge performance once in use.

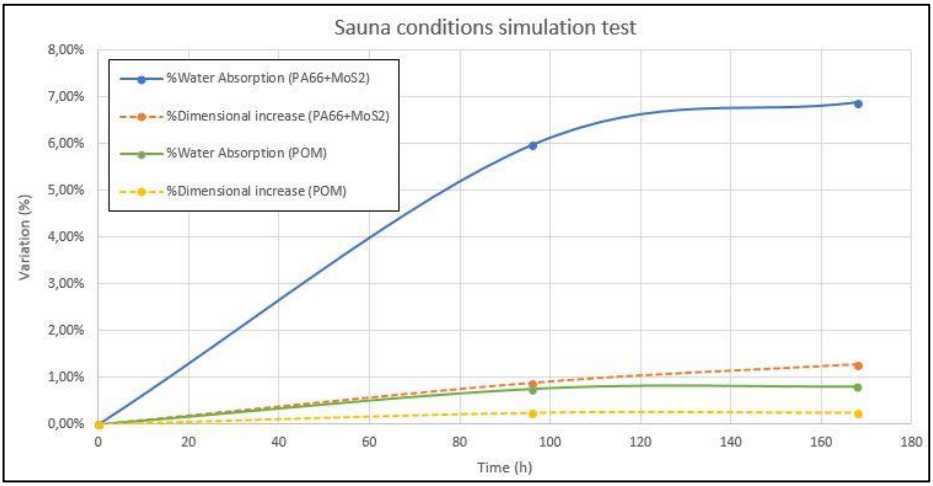

*Figure 1. Dimensional increase and water absorption for PA66+MoS_2 and POM under sauna conditions simulation test (**67**)*

4.2. PROJECT SCOPE

All the mass production cartridges use POM - POM or PA66+MoS2 - POM combination in the racord/ceramic holder system, differentiating ones from others in the geometry and size due to specific mechanical or applicability requirements. To fix the geometry and size parameters, the tests, figures and considerations are referred to the components of an ENDURA SN-35 S/D - EVO1 cartridge, seen in *Figure* **2**.

The tests have been done trying to simulate the cartridge's and its components' requirements in field, so they do not correspond to normalized tests. The theoretical and experimental outputs can only be read as comparative results between different raw materials in this concrete application.

5. INTRODUCTION

Tribology is the science that studies the behaviour of multiple surfaces working in contact. When relative movement between them is present, tribology involves friction and wear. Both phenomena depend on parameters such as the pressure applied and the sliding velocity of the system, as well as surface's roughness and the use of lubricants.

Friction (F_f) is the force that opposes to the relative movement between surfaces, on either before starting the movement (static friction) or while moving (dynamic friction). In equal conditions, the friction of a system can be compared by comparing its friction coefficient (μ), since a higher μ lead to a higher friction. Thus, a minimum friction coefficient is desired.

Wear rate (K) is defined as the volume of material loss per distance covered when two or more surfaces friction against each other's. It depends largely on the load, the velocity and the nature of the materials. In polymer-polymer combinations adhesion is the dominant wear mechanism [3]. Also, a minimum wear rate is desired.

The pressure (P) and the velocity (v) determine the PV factor, which is the product of both. It exists a PV limit above which surfaces can no longer work as a tribological system due to catastrophic wear or overheating [5], e.g. The PV factor has been constant for all the tribological tests done in the current project.

In thermoplastic pieces produced by injection moulding, the roughness of their surfaces depends largely on the mould surface roughness and the injection parameters [6]. All the pieces tested in the project were injected in the same one-cavity mould, and with the injection parameters counselled by suppliers. This does not mean that roughness is the same for each raw material, but its impact on the friction coefficients measured in the experimental tests is proportional to the one expected for pieces in mass production. In this way, roughness can be considered as a fixed parameter with no influence on the results.

5.1. MIXER CARTRIDGES

Nowadays, the most used and extended way to regulate the water flow and temperature in faucets is by using a mixer cartridge as the one observed in *Figure* **2**. It is a general-purpose item barely known by the customer, but the faucet's behaviour depends largely on its performance.

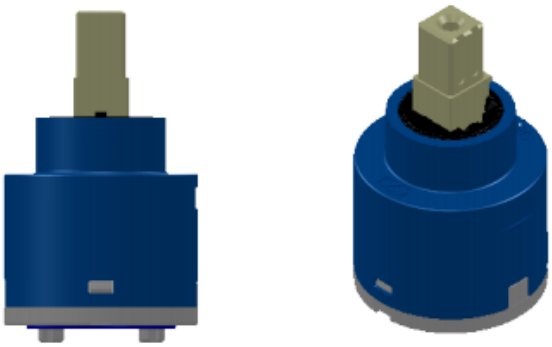

Figure 2. Assembled ENDURA SN-35 S/D - EVO1 cartridge 3D

As seen in *Figure* **3**, the cartridge is made of multiple thermoplastic components along with two alumina discs, a metal pin and elastomeric seals. There are different combinations of materials depending on the type of cartridge and its functional requirements. Concretely, in the cartridge of study, the thermoplastics used are those shown in *Table* **1**.

Table 1. Base materials for the thermoplastic components in an ENDURA SN-35 S/D - EVO1 cartridge

	Housing	**Lever**	**Racord**	**Ceramic holder**	**Base**
Material	PBT+ 15%GF (***65***)	PA6+ 30%GF (***65***)	PA66+ MoS_2	POM	PPE/PS+ 20%GF (***65***)
Grade	Bada Badadur PBT8	DSM Akulon K224-G6	Bada Badamid A70	Celanese Hostaform C9021	Sabic Noryl FE1520PW

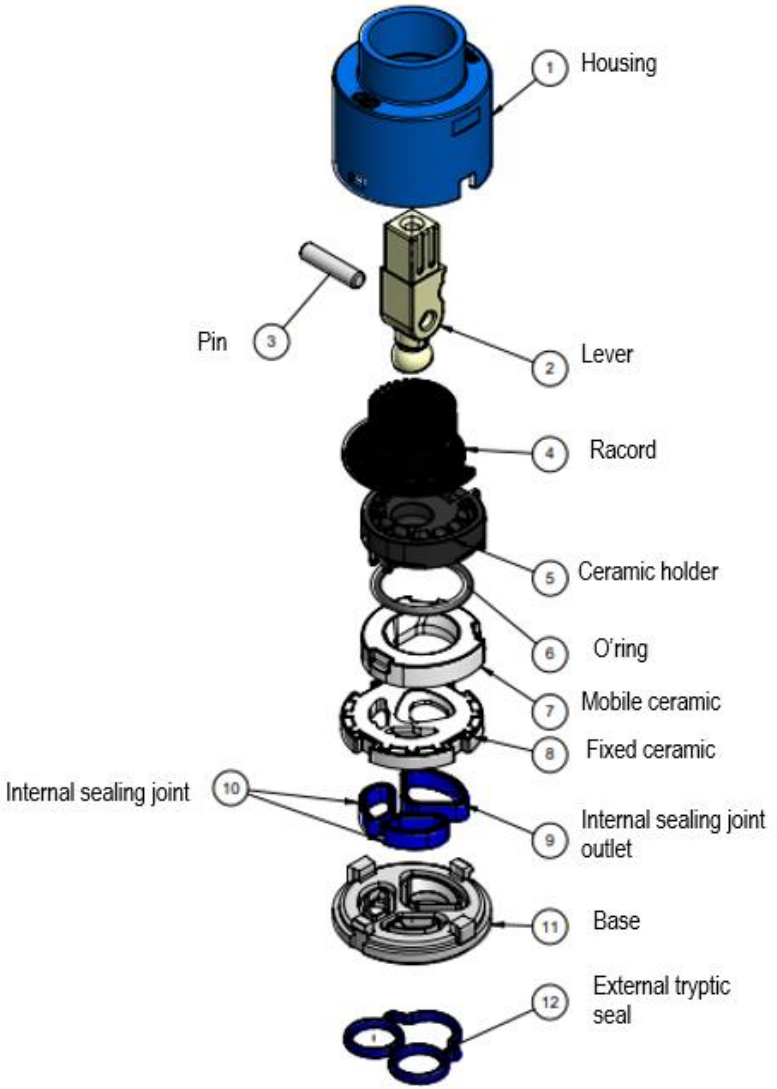

Figure 3. Components of an ENDURA SN-35 S/D - EVO1 cartridge

As seen in *Figure* **4**, the fixed ceramic has one outlet hole and two inlet holes, one for hot water and one for cold water. The relative superimposition between these three holes and the mobile ceramic's hole is what govern the water flow that passes through the faucet.

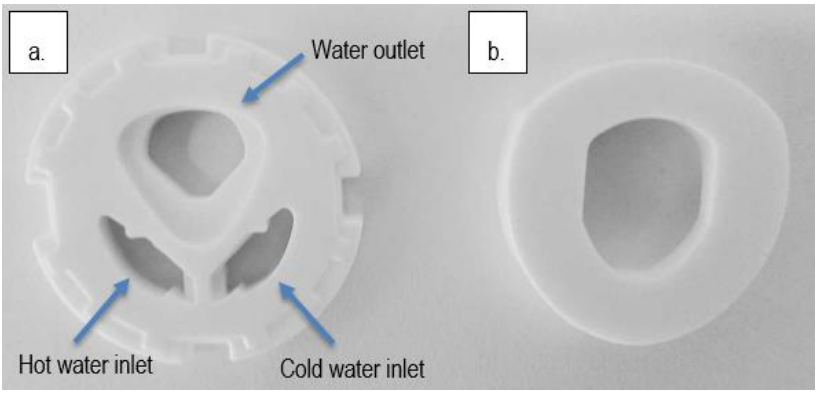

Figure 4. Top view of the ceramic discs (a) Fixed ceramic. (b) Mobile ceramic.

By operating the handle, both an aperture and a rotation angle can be applied to the lever, which transmits the movement to the ceramic holder and so to the mobile ceramic. The water flow is adjusted with the aperture angle, which can be set from 0º up to 25º (***69***). The temperature is determined by the volumetric fraction of cold and hot water, and can be regulated with the rotation angle, which can be set from -45º (total hot) up to +45º (total cold) (***69***)

When the lever is in totally vertical position, as seen in *Figure* **5** (a), the mobile ceramic's hole is superimposed exclusively on the fixed ceramic's outlet hole, not allowing water to flow through the inlets, see *Figure* **5** (b). Rotating the lever along the vertical axis, the ceramic holder does not move, so nor the ceramic discs.

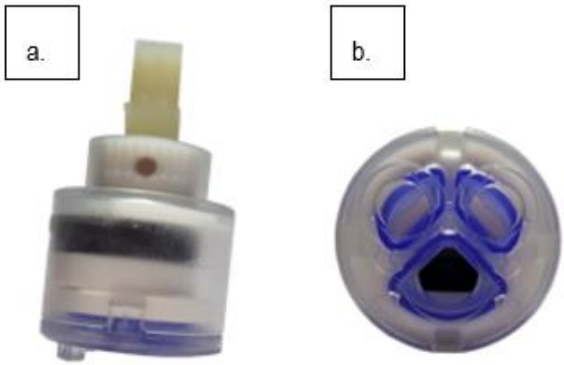

Figure 5. Lever at none aperture angle position (a) Profile view. (b) Plan view

At its maximum aperture angle, which is 25º, the mobile ceramic's hole is superimposed on both the inlet and the outlet holes equally, as seen in *Figure* **6**.

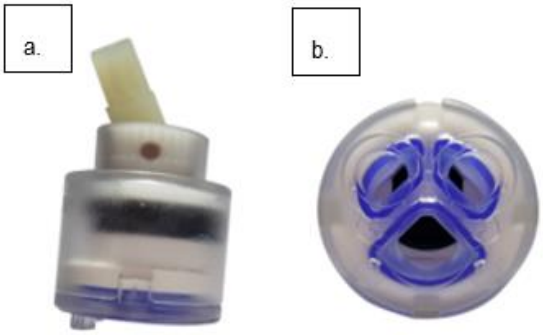

Figure 6. Lever at maximum aperture angle position (a) Profile view. (b) Plan view

Figure **7** shows how the superimposition changes by rotating the lever at its maximum aperture angle, varying the temperature as user pleases.

Figure 7. Varying the superimposition of the inlets and outlet from left (totally hot water) to right (totally cold water)

5.2. OBJECTIVES

The aim of the current project is to enhance the cartridges' tribological behaviour by improving the thermoplastic combination between the housing, the racord and the ceramic holder. Hence, it consists on carry out a theoretical selection process of those raw materials than can fit better with the requirements specified and, once determined the top candidates, contrast with empirical tests which is truly the best solution. For that purpose, the specific objectives to accomplish during the project are the following:

- To state an optimum selection procedure, what implies to analyse the system's setting and determine its contour conditions.
- To carry out internal tests about mechanical properties and dimensional response associated to water absorption and thermal expansion in order to sift the candidates.
- To determine the best candidates.
- To adapt the ball-on-disc device to the sample's geometry.
- To study the frictional and wear performances for all the relevant combinations from between the candidates.

6. CANDIDATES SELECTION PROCESS

6.1. SELECTION PROCEDURE

As mentioned, the studied system is the one formed by the housing, the racord and the ceramic holder, shown in *Figure* **8**, since the contact zones between these components are the most sensitive to friction and wear phenomena due to the presence of permanent load and relative movement. *Figure* **9** shows clearly those zones in where tribology behaviour is relevant.

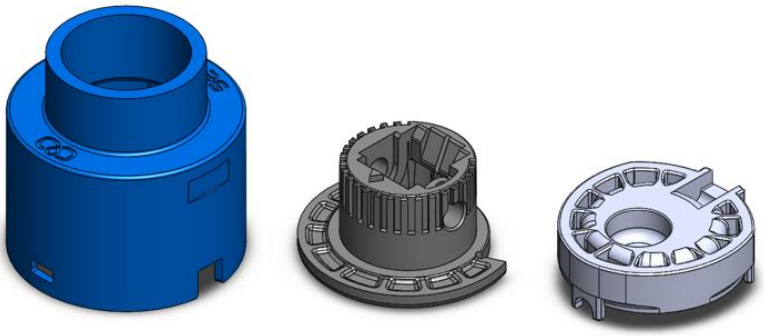

Figure 8. From left to right: housing, racord and ceramic holder

Nevertheless, all these components must accomplish other specific restrictions depending on their features. To optimize the selection process of the best polymeric combination, in the present project a first selection stage considering the requirements alien to the tribology phenomena is stated. Friction and wear tests have been done only to those candidates that have highlighted in the previous stage.

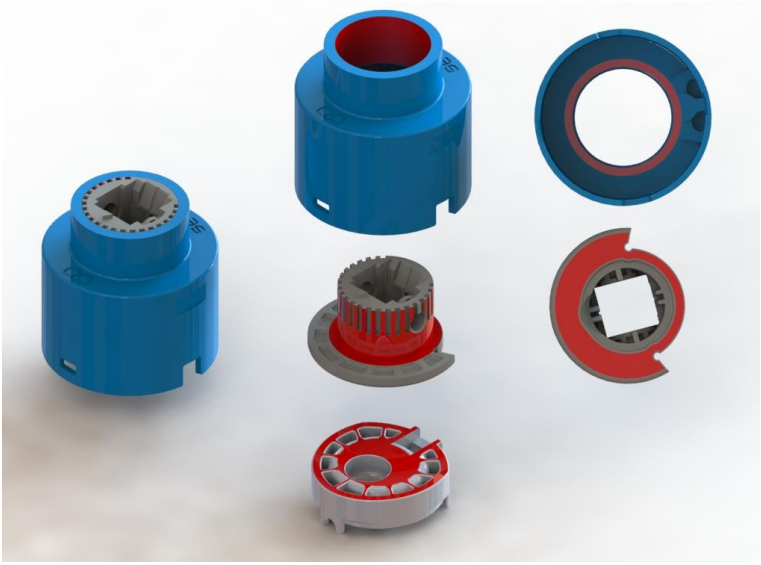

Figure 9. Isometric and plan views of the studied components. In red, those contact zones sensitive to friction and wear

6.2. HOUSING

6.2.1. Contour conditions

The housing is a structural item whose function is to compress the cartridge and keep its components in their functional position. Its currently raw material is polybutylene terephthalate (PBT) +15%GF grade Badadur PBT8, by Bada. Its function is mainly structural, and the first step in the selection process is to define those working conditions to which the housing is subjected.

Apart of the tribological behaviour against the racord, the housing targets are to display optimal resistance and low creep. Badadur PBT8 accomplish with no problems the mechanical demands, but it has some troubles facing the creep phenomena.

In summary, the current selection is based following the contour conditions showed in **Table** 2.

Table 2. Contour conditions for a housing

Function	Tubular column working under compression
Objective	Maximize the creep resistance per cost unit
Restrictions	Maintain the existing mechanical properties, Dimensions, Injectable thermoplastic
Free parameters	Raw material

6.2.2. Creep resistance

Creep phenomenon is a time-dependent deformation showed by a material when works under a constant applied stress. Among physical models for creep of polymers, the four-element Burgers model has been often used [7]. It consists on connecting a Maxwell unit and Kelvin unit in series, as shown in *Figure* **10**. In the Maxwell configuration, a spring and a dashpot are connected in series, so both are subjected to the same stress but are permitted an independent strain. In the Kelvin configuration, the two elements are connected in parallel so both are subjected to the same strain but different stress [8].

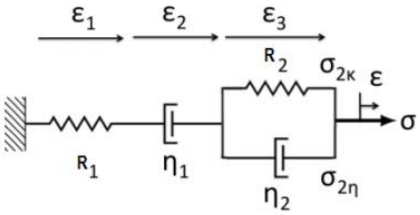

Figure 10. Burgers model (four element model) [9]

The Burgers model divide the creep strain of a polymer material into three parts: instantaneous deformation (*Eq*.**1** where $\varepsilon(t)$ in the creep strain, σ is the stress, t is time, E_1 and E_2 are the elastic moduli of the Maxwell and Kelvin springs and η_1 and η_2 are viscosities of the Maxwell and the Kelvin dashpots), viscoelastic deformation (*Eq*.**2**, which is the derivative of *Eq*.**1**) and the viscous deformation (*Eq*.**3**, where ε_0 is the instantaneous strain and *a* and *b* are material constants) [7]

$$\varepsilon(t) = \frac{\sigma}{E_1} + \frac{\sigma}{E_2}\left[1 - exp\left(-t\frac{E_2}{\eta_2}\right)\right] + \frac{\sigma}{\eta_1}t \quad (1)$$

$$\frac{d\varepsilon(t)}{dt} = \frac{\sigma}{\eta_2}\exp\left(-t\frac{E_2}{\eta_2}\right) + \frac{\sigma}{\eta_1} \quad (2)$$

$$\varepsilon(t) = at^b + \varepsilon_0 \quad (3)$$

These three parts are also known as primary, secondary and tertiary stages of the creep. As can be observed in *Figure* **11** the primary stage begins the moment the load is applied, during which deformation increases rapidly and slows with time. Secondary stage shows almost a constant and uniform deformation. In the tertiary stage, deformation increases quickly until the material's failure. The length of each stage depends on the load applied [10].

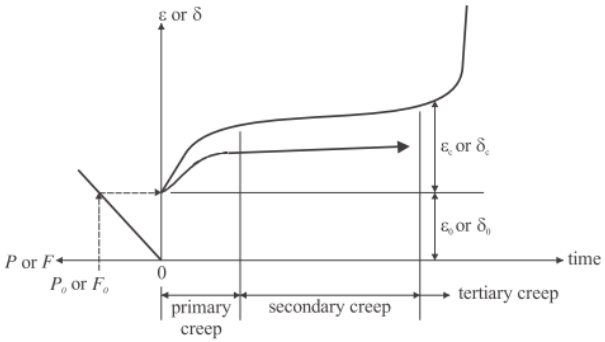

Figure 11. General description of material creep behaviour [10]

To know the creep behaviour of those materials mostly used in the housing, Sedal performed an internal test with its final geometry. In the current project, the results of this test are considered as the most reliable source of information about creep in housings. The test consisted on assembling some samples of housings injected with PBT+15%GF, blend of polyphenylene ether (PPE) and polystyrene (PS) PPE/PS+20%GF grade Noryl FE1520PW by Sabic and POM+20%GF grade Hostaform GV1/20 by Celanese to a faucet, measuring the torque needed to achieve a specified mark. The system rested 72 hours at 45ºC. After that, the torque needed to disassembly the housing was checked. The difference between the assembly and the

disassembly torque is considered as the torque loss for each material. *Table* **3** shows the test results.

Table 3. Torque loss test results

Raw material	PBT+15%GF	PPE/PS+20%GF	POM+20%GF
Mean assembly torque [N·m]	10,3	10,3	9,6
Mean disassembly torque [N·m]	4,8	7,9	5,1
Mean torque loss [%]	53,2	22,9	46,9

The results show that the material with a higher resistance to torque loss is PPE/PS+20%GF. Hence, if it fulfils the mechanical requirements, it can be considered as a potential candidate to be tested along with PBT+15%GF.

6.2.3. Mechanical demand

The size of the cartridges is determined through the diameter of the housing, which is 35 mm for the ENDURA SN-35 S/D - EVO1 cartridge's. Following EN 817:2008, cartridges are demanded to withstand a torque 6 N·m when assembled to the faucet [11]. Yet, most of the customers request the cartridge to resist a nut bolted at 12 N·m of torque. To calculate the compression that this torque represents on the cartridge, a simulation as observed in *Figure* **12** has been done. The dynamometer supports the full weight of the cartridge to be capable of determine the compressive force as the torque is applied.

Figure 12. Device used to measure the compressive force generated when the torque is applied

A Chatillon DFIS100 is the dynamometer used during the simulation. Unfortunately, its working range is up to 540 N, force which for the system is achieved with a torque of 5 N·m, obviously not sufficient. Therefore, different measurements have been done trying to estimate a trend equation. After some trials, the average compressive force depending on the torque applied is shown in *Figure* **13**.

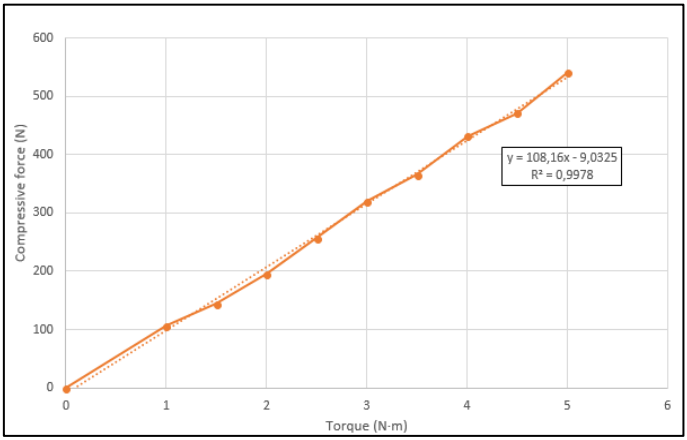

Figure 13. Representation of the compressive force according to the torque applied

As the nut taps, the contact surface between threads increases, what causes that a higher torque is needed to overpass the constantly growing static friction. In consequence, not the total of the torque applied is transferred to the cartridge in form of compressive force. Hence, the worst case for the system is to consider it is going to follow the represented linear path, according to which the estimated maximum compressive force for the cartridge in use is 1289 N.

It has been proved that the three raw materials support this compression without problems[1]. Anyway, to minimize the buckling and maximize the resistance is always desirable. From *Eq*.**4**

[1] None of the housings have failed when assembled in real field conditions, supporting the compression widely

and *Eq.***5**, where F_c is the critical force, n is the half-wavelengths in buckled shape, I is the moment of inertia, L is the length, M is the bending moment, Ze is the elastic modulus of the section and σ_{LE} is the elastic limit and with all the geometrical parameters fixed, the resulting material indices are $M_1=E$ and $M_2=\sigma_{LE}$.

$$F_c = \frac{n^2 \pi^2 EI}{L^2} \tag{4}$$

$$M = Z_e \sigma_{LE} \tag{5}$$

To maximize both indexes, a trade-off has been done. The considered mechanical properties are those given by the suppliers in the respective technical data sheets (TDS). *Figure* **14** is the plot of the material indexes revers, giving information about which is the best candidate.

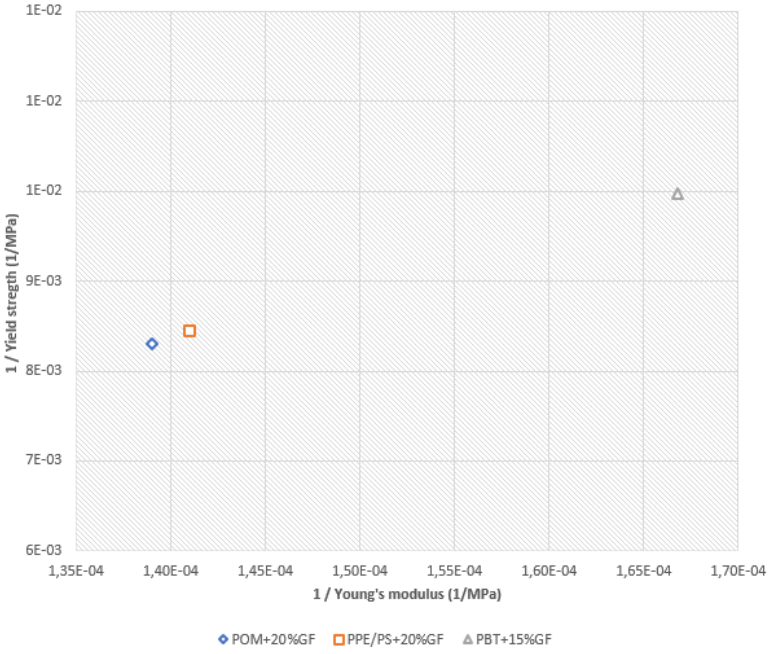

Figure 14. Trade-off between material indexes M_1 and M_2 for the candidates

It can be observed that POM+20%GF is the raw material with the best stiffness and resistance, followed closely by PPE/PS+20%GF.

Considering creep resistance, mechanical demand and the prices of the raw materials, a selection matrix has been done, as shown in *Figure* **15**. A score from 0 to 10 has been given to each candidate in function of their performance in fulfilling all the requirements.

	Creep resistance	Mechanical demand	Price	Total score
PBT+15%GF	4	5	9	5,7
PPE/PS+20%GF	8	8	7	7,7
POM+20%GF	5	9	9	7
Pondaration (%)	50	20	30	___

Figure 15. Housing's raw material selection matrix

The final decision is to include PPE/PS+20%GF in the tribological test as a candidate for become the housing's raw material.

6.3. RACORD

The current project is motivated mainly in the racord's frictional performance, as it is the piece that works between the housing and the ceramic holder and showed several issues in some cartridges. However, the racord must accomplish other requirements apart from a good tribological behaviour. It works coupled to the lever by the metallic pin and it is the responsible of limiting the rotation movement by interference with the housing.

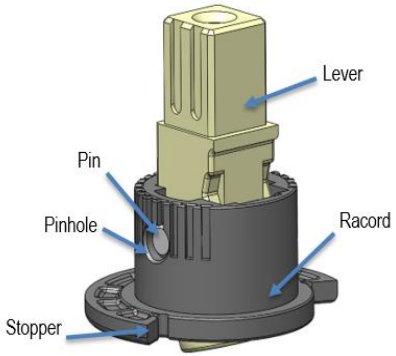

Figure 16. Representation of an assembled lever-pin-racord system

When a torque is applied to the lever, a force transmission chain is generated. It is transferred from the lever to the pin, from the pin to the pinholes, and from them to one of the interference zones between racord and housing, called stoppers (see *Figure* **16**).

When a stopper and the housing interact, both zones are subjected to the compressive force equivalent to the torque applied by the user. It has been noticed that the stoppers of the racord are the zones that suffer the most while this kind of force is applied, even entailing permanent deformation and so the failure of the racord and the cartridge. A representation of the forces implied during the contact is showed in *Figure* **17**. The dashed lines, which are tangent to the circular section and perpendicular to the application of the force, limit an approach of the section tasked to withstand the force. In that way, stoppers can be considered as beams with a non-continuous section loaded in bending. Emphasize in that only one stopper performs at once.

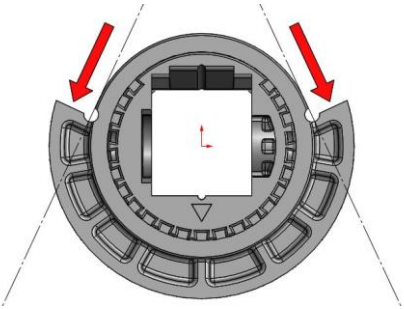

Figure 17. Representation of the force applied to the stoppers and their functional section

It is usually a requirement demanded by the costumer that the racord must be able to stand a torque of 12 N·m. The pression this torque represents for the stoppers can be calculated with *Eq.***6** I *Eq.***7**, in which *T* is the torque, *F* is the force, *P* is the pressure and *A* is the area. '*r*' refers to the distance between where the torque is applied and where the force must be supported. Hence, in this case, *r* is considered as the distance between the middle of the stopper and exactly the middle of the pin, which is in the same axis where the torque is applied.

$$T = F \cdot r \tag{6}$$

$$P = F/A \tag{7}$$

Thus, with an area of 6,75 mm^2 for each stopper, the generated pressure is 128 MPa. To understand the effect of the pressure on the stoppers and estimate their failure manner, a finite element analysis (FEA) has been done. *Figure* **18** shows the response of the racord when an instant pressure of 128 MPa is applied to one of the stopper's surface, while fixing the pinholes. *Figure* **18** (a.) represents von Mises' stress that can be generated during the maximum force application instant. The racord's geometry presents a radium between the stopper and the circular section in order to minimize the stress concentration in the zone. Yet, it is the most requested location, and in which the racord usually failures. *Figure* **18** (b.) represents the deformation suffered per location when the force applied is maximum, considering the racord does not failure before this moment. *Figure* **18** (c.) shows the zones susceptible to suffer the highest von Mises' stress and where a factor of safety makes sense. These zones clearly match with those approached in *Figure* **17**.

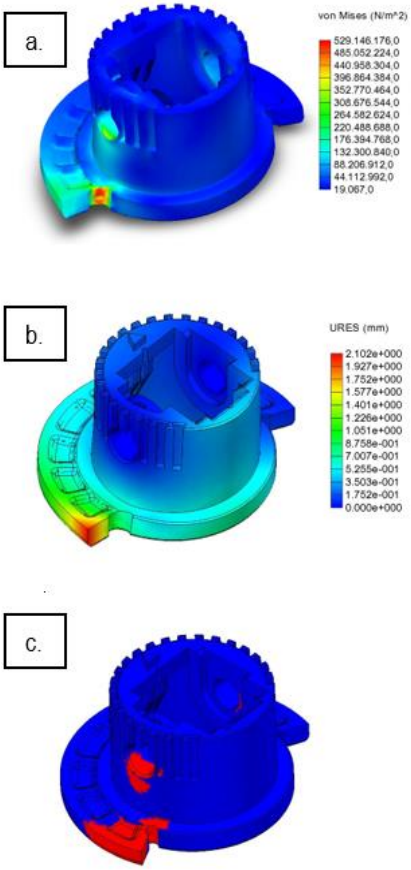

Figure 18. FEA simulations in terms of (a) von Mises' stress (b) deformation and (c) factor of safety

The racord is not only demanded to have a good mechanical performance, but another critical parameter in this application is the dimensional stability associated to humidity absorption and thermal expansion. The tolerances between the racord and the housing's neck are 0,05 mm, and if the racord growths enough the mixer could block by interference.

In field, neither POM nor PA66+MoS_2 have shown problems to achieve the mechanical requirements studied above. Essentially, the potential raw material for this concrete application should have similar or improved mechanical properties, better frictional behaviour and higher dimensional stability in humid environment. Hence, to maximize the resistance and the stiffness

is not the main objective, but it is also hugely desirable. To compare both criteria, CES EduPack2017 selection software has been used. *Figure* **19** shows the representation of those injectable thermoplastics ordered depending on its Young's modulus (*E*) and yield strength (*σe*). The axis shows the inverse of the mechanical properties to represent both objectives in a plot. As it is considered the stiffness and the resistance have the same importance in our application, a line with a slope of -1 is plotted, with the objective of minimize the index. The materials currently used in the racords are highlighted in blue. After considering other critical parameters such as availability of suppliers and the experience injecting those materials, the selected materials for the purpose of being studied were those highlighted in yellow.

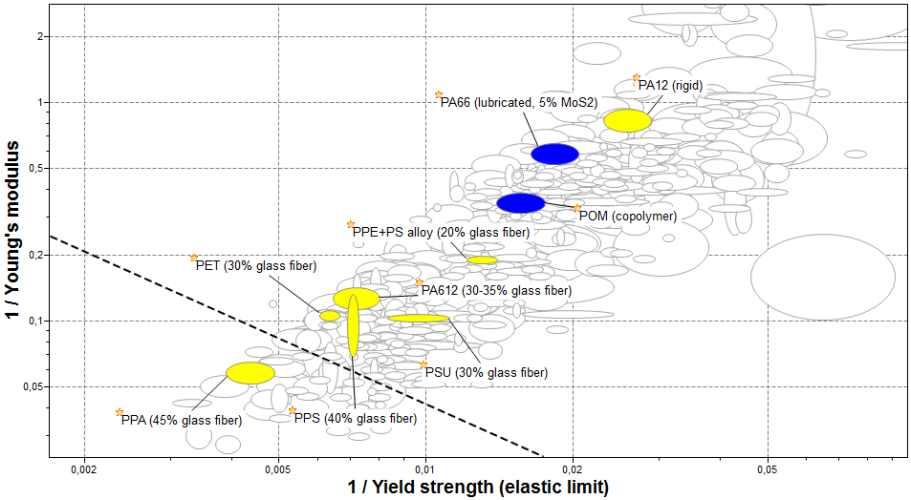

Figure 19. Relation between the inverses of E and σe for the selected candidates[2]

[2] Chart made with CES EduPack 2017 software

The racord's raw material selection must be really demanding as the final decision may be applied to mass production. That is why price is also a variable to consider. *Figure* **20** shows the representation of the product of E and σe per cost unit. Again, it is considered the mechanical properties have almost the same weight in the selection process as the price, and so the line plotted has a slope of -1.

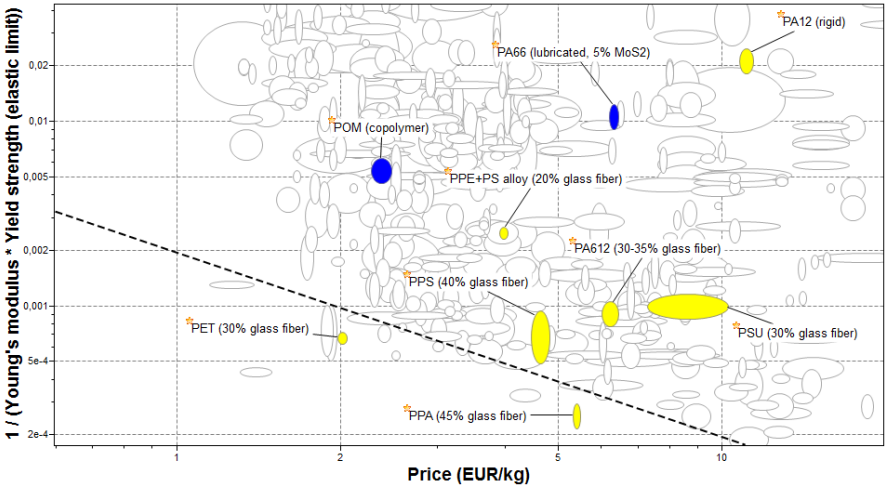

Figure 20. Relation between the inverse of the product of E and σe and the price for the selected candidates[3]

In both figures can be appreciated that the selection has been done trying to enhance both mechanical and economic values, except for polyamide 12 (PA12) (***65***), which was anyway selected with the thought it had good tribological behaviour.

Moreover, after a characterization process of a competitor's racord, have been found that polytrimethylene hexamethylene terephthalamide (PA6-3-T) (***65***) with 40% glass fibres reinforce

[3] Chart made with CES EduPack 2017 software

is used. Thus, this material is also considered as a candidate[4]. In summary, the selected materials to be injected and tested are those showed in *Table* **4**.

Table 4. Raw materials injected and tested

Material	**POM**	**PA66+MoS_2**	**PPE/PS+20%GF**
Grade	Hostaform C9021 (Celanese)	Badamid A70 (Bada)	Noryl FE1520PW (Sabic)
Material	**PSU+30%GF** (*65*)	**PA12**	**PA12+30%GF**[5]
Grade	Udel P-1700 (Solvay)	Badamid PA12 H (Bada)	Vestamid L1930 GD30 (Evonik)
Material	**PET+30%GF** (*65*)	**PA6-3-T**[6]	**PA6-3-T+35%GF**
Grade	Rynite 530 (DuPont)	Trogamid T5000 (Evonik)	Trogamid T-GF35 (Evonik)
Material	**PPA+40%GF** (*65*)	**PPS+40%GF** (*65*)	**PA6.12+30%GF** (*65*)
Grade	Grivory GV-4H (EMS)	Fortron 9141L4 (Celanese)	Radilon DT RV300RKC2 (Radici)

6.3.1. Mechanical tests

Torque resistance tests have been done to compare the candidates. The tests were all done in exactly the same conditions, and with the procedure shown in *Figure* **21**.

[4] The PA6-3-T grade tested is filled with 35%GF
[5] PA12 filled with 30%GF has been also tested
[6] PA6-3-T unfilled has been also tested

Figure 21. Torque resistance test procedure

A score from 0 to 10 has been given to each raw material in function of their performance with the objective to create a matrix that help in the decision, shown in *Figure* **24**.

6.3.2. Dimensional stability

The dimensional increase of the racord is such a critical factor that boosted the current project when it was observed that PA66+MoS2 had the potential risk to block the cartridge. The dimensional variation may occur due to two main causes, the moisture absorption and the thermal expansion. Some tests have been done to compare the candidates' performance in both aspects.

6.3.2.1. Dimensional increase associated to moisture absorption

Every thermoplastic has an own moisture absorption percentage, which is nearly the long-term absorption percentage at 23ºC in a 50% relative humidity atmosphere usually given by the producer [12]. As in some TDS this associated percentage is calculated following different standards or may not be given, an internal experimental test has been conducted. Moreover, in order to speed up the test, the racords have been submerged in hot water at 60ºC for 6 hours [13]. Initial, final and in-between measures of weight and dimensions have been done. *Figure* **22** shows the water absorption for all the candidates.

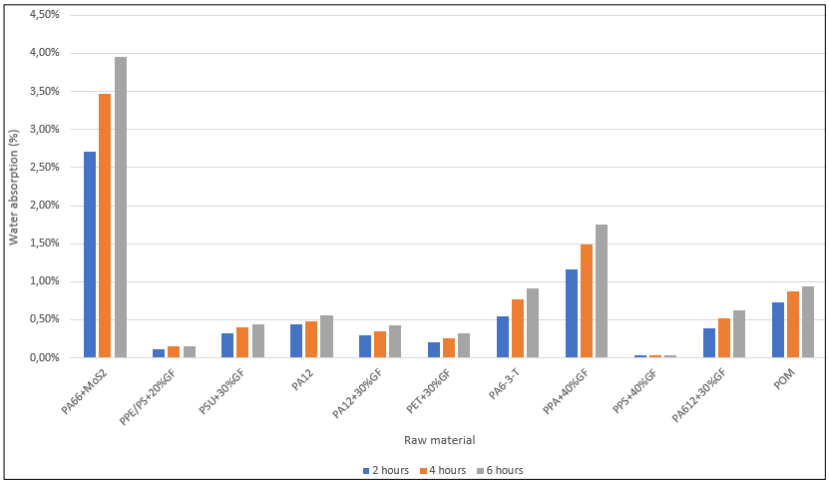

Figure 22. Percentage of water absorption measured for each raw material after two, four and six hours submerged

Although the moisture absorption is an important parameter and can provide a near idea of which of the candidates are the best, what is really important for the racord's raw material is the dimensional increase associated to this percentage. The test has proved that for an equal moisture absorption percentage, the dimensional increase varies depending on the type of thermoplastic. *Figure* **23** shows this tendency for each raw material.

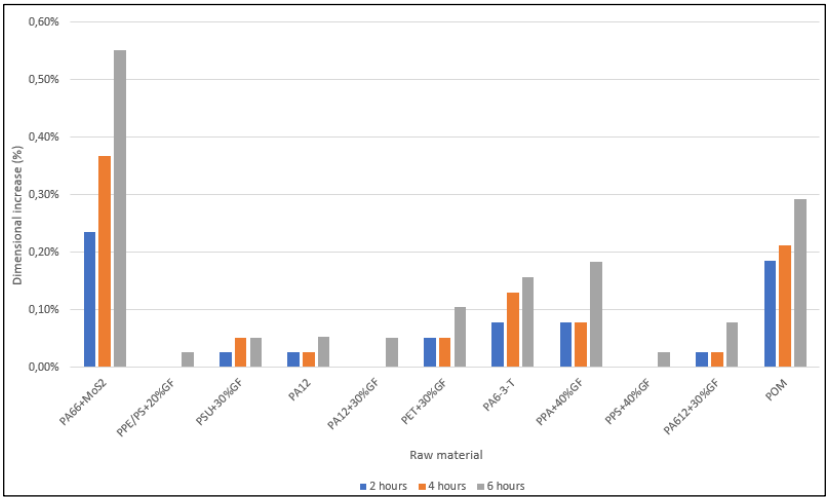

Figure 23. Dimensional increase for each raw material after two, four and six hours submerged

A score from 0 to 10 has been given to each raw material in function of their performance with the objective to create a matrix that help in the decision, given in *Figure* **24**.

6.3.2.2. Thermal expansion

Cartridges are demanded to work in humid environment but also at temperatures that may reach 60ºC. In these cases, a high thermal expansion may lead to an excessive dimensional increase and so to a cartridge block. To compare this parameter in the racord's final geometry, some samples of each raw material have been measured at 24ºC and at 60ºC. With *Eq*.**8**, in which ΔL and ΔT are the dimensional and temperature increase, respectively, the thermal expansion coefficient (α) has been calculated for all of them.

$$\Delta L = L \cdot \Delta T \cdot \alpha \quad (8)$$

The results are shown in *Table* **5**.

Table 5. Thermal expansion coefficient measured for each candidate

Material	**POM**	**PA66+MoS_2**	**PPE/PS+20%GF**
α [1/K]	9,48E-5	4,38E-5	2,54E-5
Material	**PSU+30%GF**	**PA12**	**PA12+30%GF**
α [1/K]	3,65E-5	6,58E-5	4,74E-5
Material	**PET+30%GF**	**PA6-3-T**	**PA6-3-T+35%GF**
α [1/K]	4,01E-5	5,47E-5	-----[7]
Material	**PPA+40%GF**	**PPS+40%GF**	**PA6.12+30%GF**
α [1/K]	3,64E-5	3,27E-5	4,20E-5

[7] PA6-3-T+35%GF based racords could not be injected due to expulsion issues during injection

To help choosing the best candidates, a decision matrix with the punctuation scored in each test has been done. *Figure* **24** shows the scores of each material and the decision about if it is a potential substitute and so if it is going to be tested in the ball-on-disk device.

	Torque resistance (0-10)	Dimensional stability (0-10)	Thermal expansion (0-10)	Cost (0-10)	Total score (0-10)	Final decision
POM	5	6	5	8	6,35	Currently used
PA66+MoS_2	6	4	9	8	6,25	Currently used
PPE/PS+20%GF	8	10	10	7	8,35	YES
PSU+30%GF	6	9	9	2	5,65	NO
PA6.12+30%GF	7	9	9	6	7,35	YES
PA12	2	9	___	4	Not resistant enough	NO
PA12+30%GF	5	9	8	4	6	NO
PET+30%GF	8	8	9	8	8,05	YES
PA6-3-T	7	7	8	4	6	NO
PA6-3-T+35%GF	___	___	___	4	___	YES
PPA+40%GF	9	7	9	7	7,7	YES
PPS+40%GF	9	10	9	6	8,25	YES
Ponderation (%)	30%	30%	5%	35%	___	___

Figure 24. Decision matrix showing the score of each material for their performance in each test. Every parameter has an associated subjective ponderation based on experience. According to the score, a final decision is taken.

Polyamide 12 (PA12) has been directly discarded after its bad performance in the torque resistance test. Instead, PA6-3-T+35%GF is still considered. Moreover, to be compared with the updated combinations, POM and PA66+MoS_2 are also selected.

6.4. CERAMIC HOLDER

The ceramic holder is the third item forming this three-pieces working under friction and wear combination. Its function is to transmit the movement applied by the user to the mobile ceramic, as both are coupled.

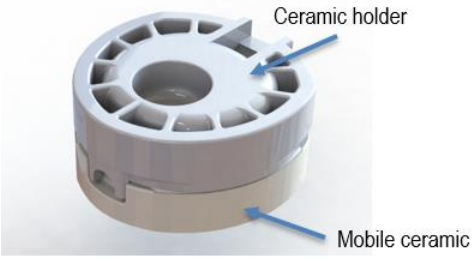

Figure 25. Assembled ceramic holder and mobile ceramic

In most of the cartridges, included the ENDURA SN-35 S/D - EVO1, ceramic holder works in contact with the water. In most of the countries, plastic materials intended to work in these conditions are demanded to have the respective official certifications. These certifications' purpose is to ensure that a product is able and safe for use in drinking water. Although each country has its own regulations, most of them derive from or even accept WRAS, KTW, NSF-61 and ACS, which are the official certifications from United Kingdom, Germany, United States of America and France, respectively.

Therefore, and because POM has good friction behaviour [1], it has been decided not to change the ceramic holder's raw material.

7. TRIBOLOGICAL RESEARCH

Once the candidates for the system have been selected, the tribological behaviour between them is studied. The final candidates potentially applicable to each item are:

- Housing: PPE/PS+20%GF and PBT+15%GF (currently used)
- Racord: Polyphenylene sulfide (PPS)+40%GF, polyphthalamide (PPA)+40%GF, PA6.12+30%GF, polyethylene terephthalate (PET)+30%GF, PPE/PS+20%GF, PA6-3-T+35%GF, POM (currently used) and PA66+MoS_2 (currently used)
- Ceramic holder: POM (currently used)

As the racord is forced to friction against POM and one of the two candidates of the housing, these three raw materials have been tested against all nine racord's candidates. Thus, the combinations that have been finally tested are shown in *Figure* **26**:

	POM	PA66 + MoS_2	PPE/PS + 20%GF	PA6.12 + 30%GF	PET + 30%GF	PA6-3-T + 35%GF	PPA + 40%GF	PPS + 40%GF	PBT + 15%GF
POM	✓	✓	✓	✓	✓	✓	✓	✓	✓
PPE/PS + 20%GF	✓	✓	✓	✓	✓	✓	✓	✓	✓
PBT + 15%GF	✓	✓	✓	✓	✓	✓	✓	✓	✓

Figure 26. Representation of all the combinations tested with the tribometer device

7.1. EXPERIMENTAL EQUIPMENT

A ball-on-disk device by *CM4 Enginyeria S.A.*, owned by *Centre de Projecció Tèrmica* (CPT) is used to measure the friction and wear between polymeric pairs. The equipment, seen in *Figure* **27**, follows standard ASTM G99-04 [14] to calculate the friction coefficient. As seen in *Figure* **28** the test consists on rotate a surface in contact with a fixed sphere with a defined velocity, load and distance to cover.

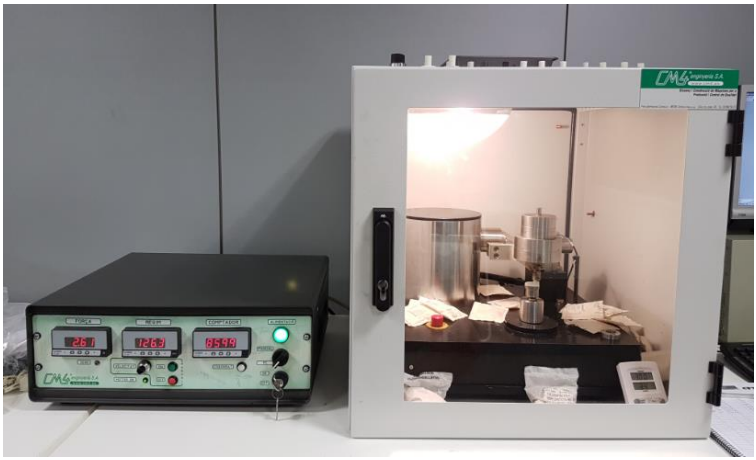

Figure 27. Ball-on-disk device

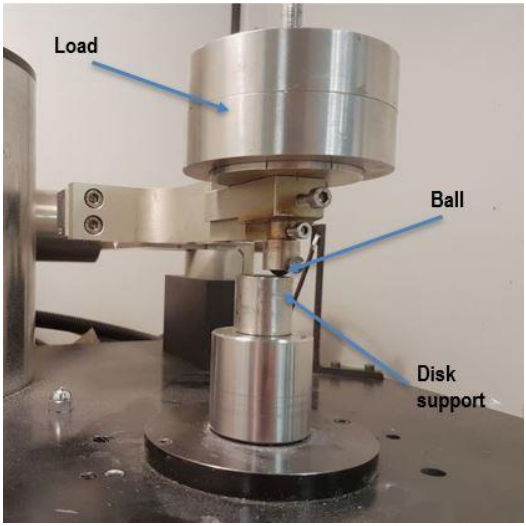

Figure 28. Original mechanism of the ball-on-disk device

7.2. ADAPTATION OF THE EQUIPMENT

As mentioned, the ball-on-disk device uses a sphere to friction against a surface, as demanded by the standard. In the majority of the tests the ball used is made of steel, WC-Co or Al_2O_3. Friction coefficients are usually given as if they were an intrinsic property of the material,

but the fact is those coefficients are, in most of the cases, measured against steel. Actually, the friction coefficient depends on the combination of the materials that are tested, among other factors. The current project's aim is to study the frictional behaviour between different polymeric pairs, so the device had to be adapted to this demand.

The original idea was to inject spheres and rectangular plates with the same dimensions as those generally used in the device. When a sphere slides against a surface, the theoretical interference between them is a point. Polymeric spheres would be in risk of suffer plastic deformation in the contact point leading to a non-constant interference zone, and so to distorted results, as that deformation would not be the same for each combination. To resolve this issue the sphere geometry has been replaced by a cylinder called pin. Pin-on-disk test is also widely used to measure friction coefficient and wear.

To make profit of an existent mould, the disk has been designed very close to the ceramic holder's geometry, but with a totally flat upper surface and significantly thinner to avoid cavities during injection. *Figure* **29** shows the designs for the pieces to be injected and a ceramic holder currently in use.

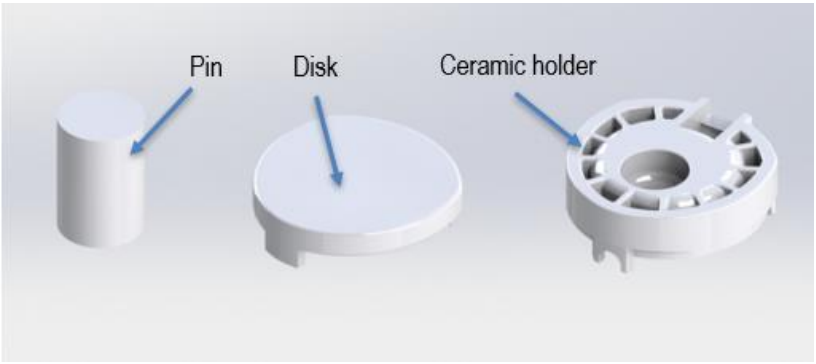

Figure 29. Isometric view of the pin and the disk designs compared to an ENDURA SN-35 S/D - EVO1 cartridge's ceramic holder

The disk's feet, similar to the original ones, have been kept to help fixing the disks to the device. To do so, a specific joining item has been designed. This item simulates the geometry of a mobile ceramic and can be joined to the pin-on-disk device by a thread. *Figure* **30** shows the design of the joining item with an assembled disk.

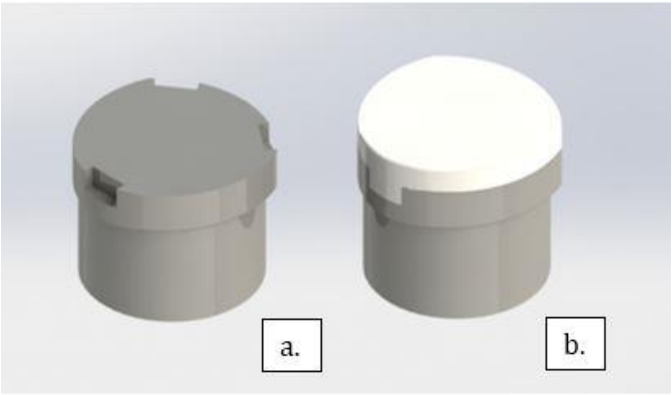

Figure 30. Isometric view of (a) the joining item & (b) a disk fixed to the joining item

Once the final geometries were designed, Sedal's mould-makers modified an existent but outdated mould to adapt it at them. *Figure* **31** shows the both faces of the updated mould.

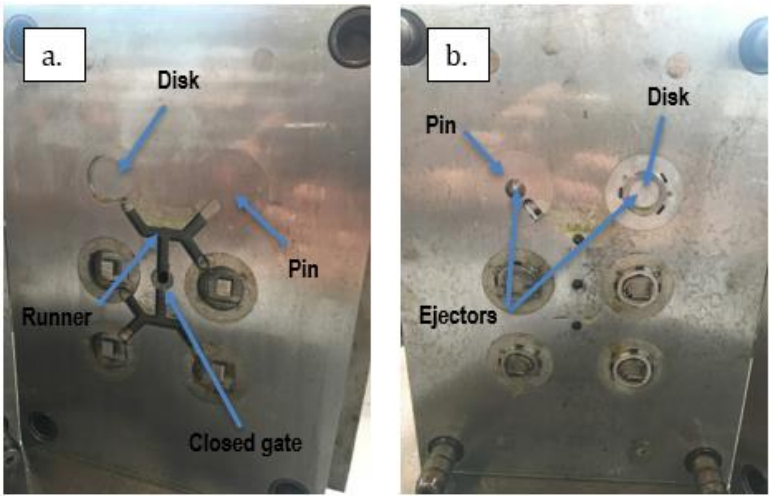

Figure 31. Primary components of a mould, (a) the injection mould and (b) the ejector mould

There is only one cavity for the pin and the disk geometries, and so all the tested pieces have been injected in the same one. The surfaces meant to be in contact during the pin-on-disk test are on the injection mould face to maximize their flatness and avoid local deformations caused by the ejectors.

Figure **32** shows a sample of a pin and a disk for each injected candidate, as well as the mechanized joining item.

Figure 32. Mechanized joining item and pins and disks made of (from top left to bottom right) PET+30%GF, PA66+MoS2, PA6.12+30%GF, PA6-3-T+35%GF , PPA+40%GF, PPE/PS+20%GF, PPS+40%GF, PBT+15%GF and POM

Once set, the pin-on-disk device adaptation works as shown in *Figure* **33**

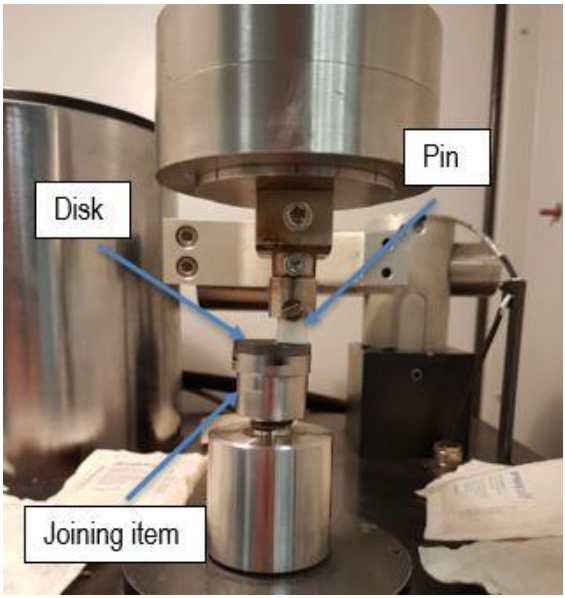

Figure 33. Modified device once set the component

7.3. EXPERIMENTAL PROCESS

Considering not only the raw material but also the geometry, a total of twenty-seven tests have been done with the tribometer.

To obtain truly comparable information about friction coefficients, the tests have been always done with disks made of POM, PPE/PS+20%GF or PBT+15%GF. To measure the effect the geometry has on the friction coefficient, crossed tests have been done between these three candidates. It means POM – PBT+15%GF combination, e.g., has been tested twice, but with swapped component's raw material; and the same for POM – PPE/PS+20%GF and PBT – PPE/PS+20%GF tests. Moreover, to measure the effect the geometry has on the wear rate, same-raw material tests have been done. In particular, POM – POM, PBT+15%GF – PBT+15%GF and PPE/PS+20%GF – PPE/PS+20%GF combinations have been tested as wear control tests.

In practice, the experimental procedure and modus operandi have been identical for all the tests, during which the following patterns have always been followed:

- Weight measures have been done for all the components before and after each test. Afore weighting them for the second time, the pieces have been cleaned with airflow to remove the potential wear debris.
- The temperature for all the tests has been 29±2 ºC. Thus, temperature is considered as a fixed parameter with no influence on the variability of the results.
- The relative humidity is controlled through silica gel. For all the tests it has been about 36±4 %. Again, it is considered as a fixed parameter with no influence on the variability of the results, apart from the particular response of each thermoplastic.
- All the samples have been kept in hermetic bags to avoid them absorb moisture from the environment.
- The *PV* factor has a strong influence on friction coefficient and wear rate. Increasing the load, the friction coefficient decreases, but only at elastic contact. If during the test plastic deformation occurs, the coefficient increases with the load [3]. To avoid any interference caused by the *PV* factor, both the contact pressure and the sliding velocity have been the same for all the tests. As specified in the standard operating

procedure (SOP) of the pin-on-disk device, the load used is 30 N and the rotating speed is 124 rpm, what for our system means a linear velocity of 0,11 m/s.

- It takes 22737 turns of the disk to finish a test, what means a total distance covered of 1000 m. The distance has been the same for all the tests.

It takes three hours for each test to finish. For most of them the friction coefficient varies significantly before stabilizing. That is why the μ, provided by the software, is measured from the average of the last 200 m.

As mentioned before, the wear rate is defined as the volume of material loss per distance covered when two or more surfaces friction against each other's. It has been calculated considering the weight loss, the density of each raw material and the distance covered. Wear rate is typically expressed in mm^3/m, what corresponds to mm^2.

8. RESULTS AND DISCUSSION

8.1. TRIBOLOGY AGAINST POM

As the ceramic holder's raw material, POM is demanded to display good tribological performance with the racord's raw material. *Figure* **34** shows the evolution of the friction coefficient during the hole test for the racord's candidates against POM, as well as the results of POM-POM and POM-PBT+15%GF combinations. As the software calculates the μ from the average of the last 200 m, when theoretically the pattern has stabilized, in (***71***) are shown the tendencies during this range. In both figures can be observed that the highest μ is given when POM slides against itself.

The obtained friction coefficients for all the candidates after sliding against POM are shown in *Table* **6**.

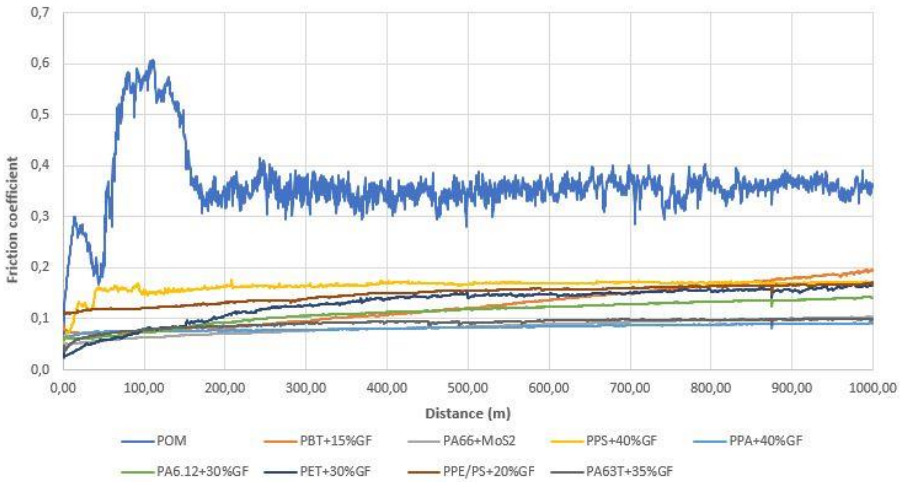

*Figure 34. Evolution of the candidates' friction coefficient in function of the distance covered when sliding against POM (**71**)*

The tests have demonstrated that POM has an excellent friction behaviour against other thermoplastic materials, except against itself. The best friction performances are those in where POM slides against polyamides family (***71***).

Table 6. Friction coefficient for each candidate against POM

Material	**POM**	**PBT+15%GF**	**PA66+MoS_2**	**PPS+40%GF**	**PPA+40%GF**
μ	0,36	0,18	0,10	0,17	0,09
Material	**PA6.12+30%GF**	**PET+30%GF**	**PPE/PS+20%GF**	**PA63T+35%GF**	
μ	0,14	0,16	0,17	0,10	

Some tests show a distinct irregular pattern, with visible marked peaks in the evolution of the friction coefficient graph. Using a POM based disk this phenomenon is only observed when using a POM based pin. It can be observed that the combinations that have this type of behaviour submit in turn the highest friction coefficients (as seen also for PBT+15%GF in *Figure* **39** and for PPE/PS+20%GF in *Figure* **43**), and all of them are associated to the highest wear rates. This phenomenon can be explained by analysing how the wear influence on polymeric surfaces in contact. As told, adhesion wear is the most common wear mechanism in these kind of combinations [3]. The process involves bonding between surfaces, plastic deformation and leads to the fracture of surface asperities, as seen in *Figure* **35**.

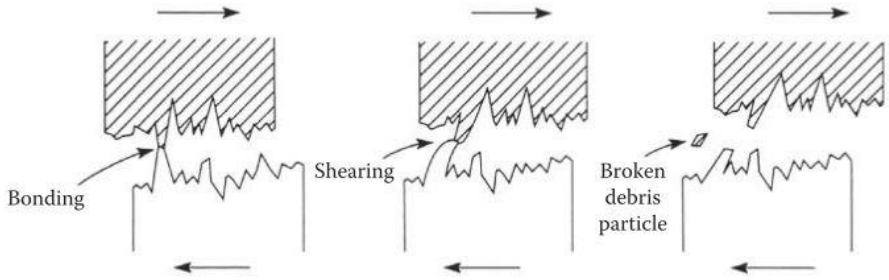

Figure 35. Representation of the processes involved in adhesive wear [15]

The broken debris asperities may form tiny abrasive particles, which if remain between the surfaces, contribute to further wear. It is the presence of these abrasive particles what induce to the peaks observed in the graph. From the information that can be extracted from the tests, the

effect the abrasive particles have on the friction coefficient can begin, vary or even stop at any time. In this way, the early behaviour of the POM-POM test could be explained in two phases. The first one is when the pin is opening a path on the disk, generating abrasive debris and plotting an accelerate increase of the μ in the graph, achieving a maximum after 100 m covered. A second phase in where no more particles are generated, and the friction coefficient is adapted to the new system, formed by two pressured surfaces with particles between them.

The highest wear rates took place when sliding against itself and PA6-3-T+35%GF. For POM based disk combinations can be observed it is not necessary to carry out a poor friction performance to cause also high wear. The average wear rate for the POM's disk is $1{,}11 \cdot 10^{-3}$ mm^2.

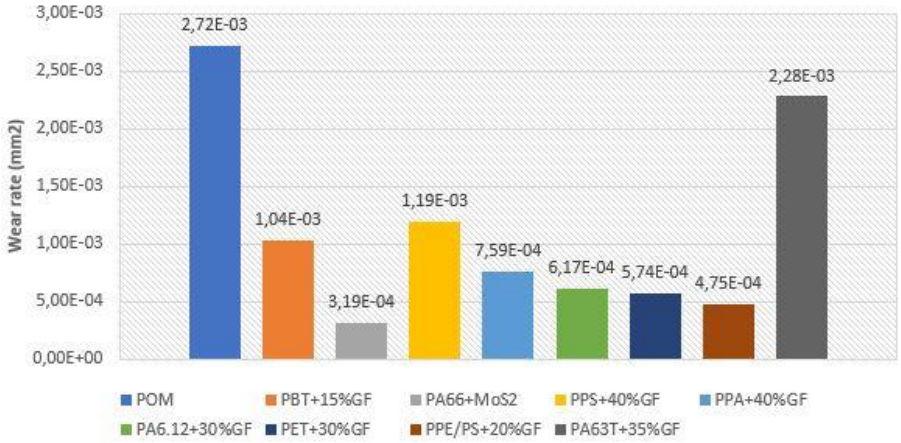

Figure 36. Wear rate caused by the candidates on POM based disk

The abrasion each combination causes on the disk is as important as the abrasion it causes on the pin. In *Figure* **37** both obtained results for all the candidates are represented. Among the racord's candidates, PPS+40%GF and PA6.12+30%GF against POM are the combinations with lowest wear. Instead, candidates that lead to a lower wear rate on the disk like PPE/PS+20%GF or PET+30%GF are more susceptible to suffer abrasive from POM.

Considering the obtained results, the candidates have been sorted from best to worst in both friction and wear qualities. The total punctuation states a priority order for compare tribology performance against a POM based disk to those displayed against PPE/PS+20%GF and PBT+15%GF based ones. As shown in *Figure* **38**, in between the racord's candidates

PA6.12+30% is the best alternative to PA66+MoS_2, nearly followed by PPS+40%GF and PPA+40%GF.

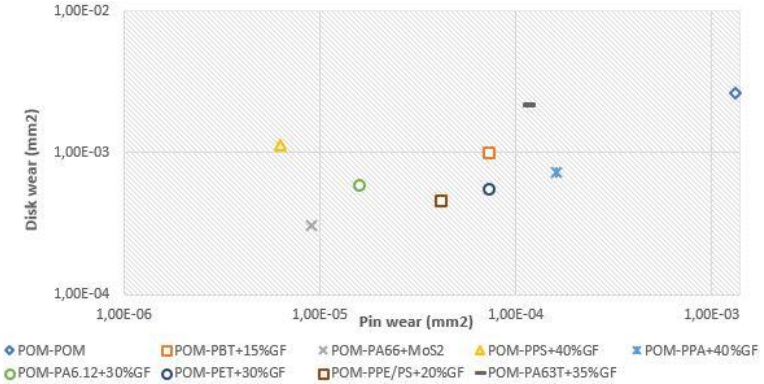

Figure 37. Wear rate caused for each combination to both pin and disk geometries for POM based disks

	POM	PBT + 15%GF	PA66 + MoS_2	PPS + 40%GF	PPA + 40%GF	PA6.12 + 30%GF	PET + 30%GF	PPE/PS + 20%GF	PA6-3-T + 35%GF
Friction coefficient	9	8	2	6	1	4	5	6	2
Wear rate	9	6	1	2	7	3	5	4	8
Total	**18**	**14**	**3**	**8**	**8**	**7**	**10**	**10**	**10**

Figure 38. Sorted candidates from best (1) to worst (9) considering friction and wear displayed against POM based disk

8.2. TRIBOLOGY AGAINST PBT+15%GF

The evolution of the friction coefficients when sliding against PBT+15%GF is plotted in *Figure* **39**, amplified in (**73**), and the values are shown in *Table* **7**.

*Table 7. Friction coefficient for each candidate against PBT+15%GF (**73**)*

Material	**POM**	**PBT+15%GF**	**PA66+MoS_2**	**PPS+40%GF**	**PPA+40%GF**
μ	0,26	0,31	0,24	0,25	0,10
Material	**PA6.12+30%GF**	**PET+30%GF**	**PPE/PS+20%GF**	**PA63T+35%GF**	
μ	0,21	0,20	0,19	0,10	

Predictably, thermoplastics sliding against PBT+15%GF display slightly worse friction perform than against POM. Polyphthalamides highlight with the lowest μ, while the highest and worst is when using a PBT+15%GF based pin. Again, sliding a polymer against itself leads to a bad frictional behaviour.

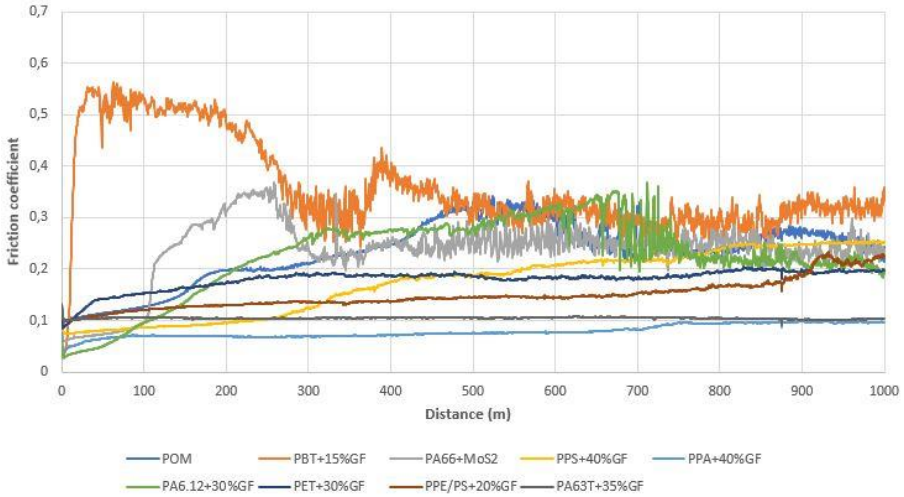

*Figure 39. Evolution of the candidates' friction coefficient in function of the distance covered when sliding against PBT+15%GF (**73**)*

The wear each material causes to the PBT+15% based disk is represented in *Figure* **40**.

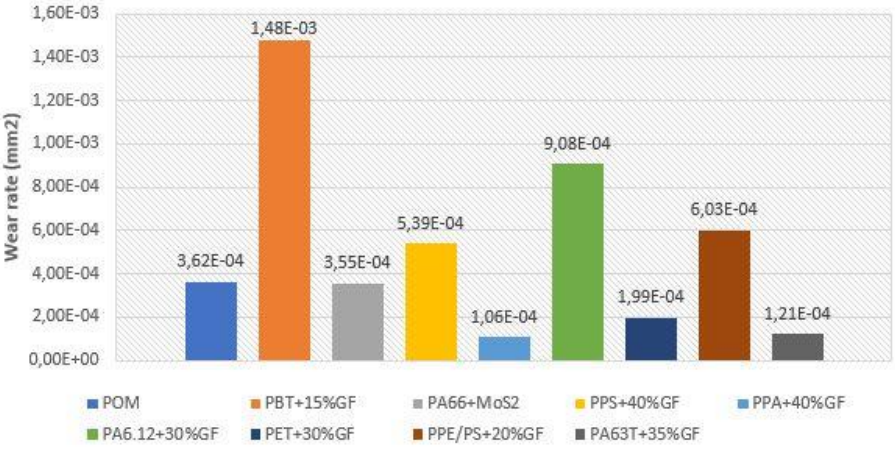

Figure 40. Wear rate caused by the candidates on PBT+15%GF based disk

The average wear rate for the PBT+15%GF's disk is $5{,}19 \cdot 10^{-4}$ mm^2, notably low.

In POM based disk case, with only one really abrasive combination, the relation between the irregular pattern and the highest wear rate is easily observable in *Figure* **36**. In the current case this pattern can be observed with PBT+15%GF, PA66+MoS_2, POM and PA6.12+30%GF. The fact in *Figure* **40** some of these combinations show a low wear rate means the most damaged piece is not the disk, but the pin. In *Figure* **41** can be observed indeed how POM and PA66+MoS_2 based pins have huge wear rate and so promoting the irregular pattern.

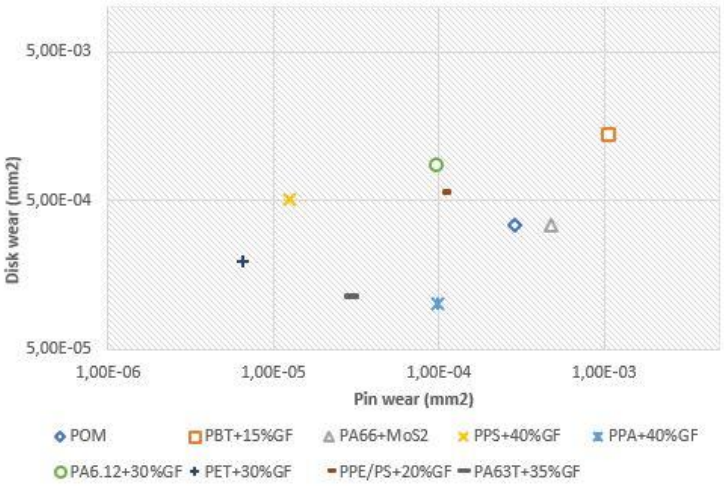

Figure 41. Wear rate caused for each combination to both pin and disk geometries for PBT+15%GF based disks

From the results, the candidates sliding against PBT+15%GF can be punctuated and sorted depending on their performance as follows:

	POM	PBT + 15%GF	PA66 + MoS_2	PPS + 40%GF	PPA + 40%GF	PA6.12 + 30%GF	PET + 30%GF	PPE/PS + 20%GF	PA6-3-T + 35%GF
Friction coefficient	8	9	6	7	1	5	4	3	1
Wear rate	7	9	8	3	4	6	1	5	2
Total	**15**	**18**	**14**	**10**	**5**	**11**	**5**	**8**	**3**

Figure 42. Sorted candidates from best (1) to worst (9) considering friction and wear displayed against PBT+15%GF based disk

The best combination to slide against PBT+15%GF is PA6-3-T+35%GF, followed by PPA+40%GF and PET+30%GF.

8.3. TRIBOLOGY AGAINST PPE/PS+20%GF

PPE/PS+20%GF is a potential substitute as the housing's raw material in detriment of PBT+15%GF. The friction coefficients measured using it as the disk material are shown in *Table* **8**, and their evolution in function of the distance covered is shown in *Figure* **43**.

*Table 8. Friction coefficient for each candidate against PPE/PS+20%GF (**75**)*

Material	**POM**	**PBT+15%GF**	**PA66+MoS_2**	**PPS+40%GF**	**PPA+40%GF**
μ	0,16	0,40	0,24	0,38	0,28
Material	**PA6.12+30%GF**	**PET+30%GF**	**PPE/PS+20%GF**	**PA63T+35%GF**	
μ	0,28	0,34	0,42	0,39	

Tests sliding against PPE/PS+20% have displayed worse values of friction coefficient than against the others. Meanwhile the average μ when sliding against POM and PBT+15%GF are 0,16 and 0,21 respectively, for PPE/PS+20%GF is 0,32.

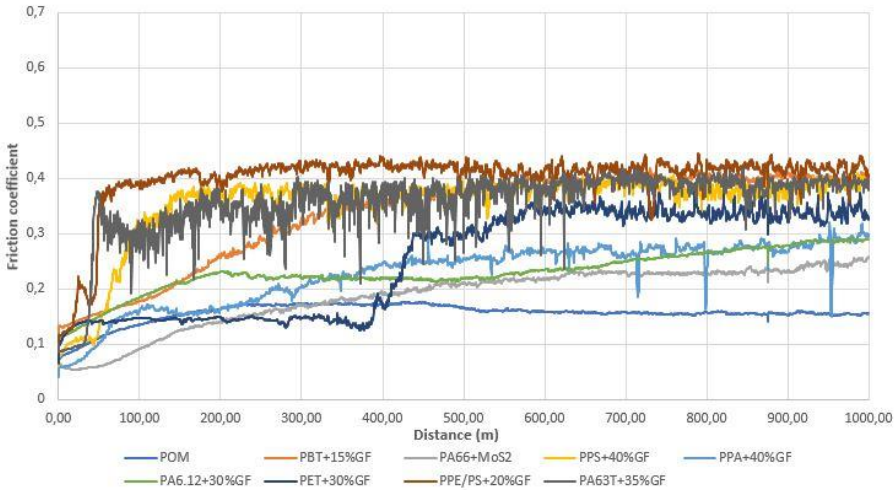

*Figure 43. Evolution of the candidates' friction coefficient in function of the distance covered when sliding against PPE/PS+20%GF (**75**)*

Combinations between PPE/PS+20%GF based disk and PPS+40%GF, PA6-3-T+35%GF and PPE/PS+20%GF itself based pins clearly follow the pattern of those most abrasive pairs. PET+30%GF based pin test demonstrates that the tiny particles can start detaching or affecting significantly the friction at any time; in this case, after 380 m covered, approximately. *Figure* **44** shows the huge difference between those most abrasive combinations and the others when sliding on a PPE/PS+20%GF based disk.

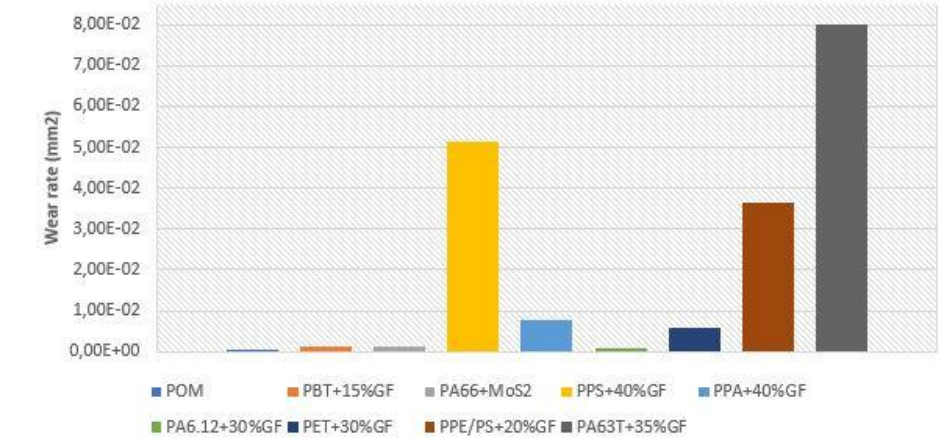

Figure 44. Wear rate caused by the candidates on PPE/PS+20%GF based disk

Figure **45** shows an amplified and quantified plot's representation.

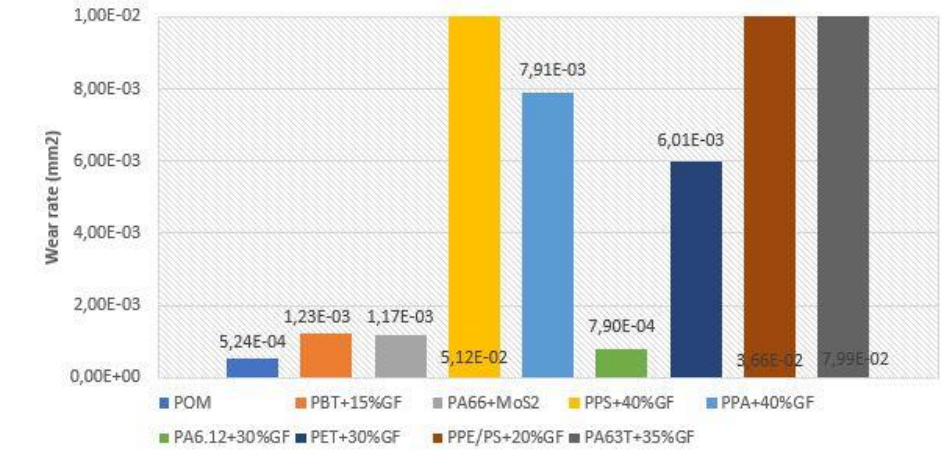

Figure 45. Amplified representation of wear rate caused by the candidates on PPE/PS+20%GF based disk

Even in the less abrasive combinations, the abrasion caused on the PPE/PS+20%GF based disks is notoriously greater than for the other studied materials. The average wear rate in the current case is $2{,}06 \cdot 10^{-2}$, what is 18 times greater than for POM and almost 40 times greater than for PBT+15%GF. Hence, PPE/PS+20%GF is the raw material most sensitive to wear from between the studied three. *Figure* **46** shows an example of the abrasion magnitude once finished a test. The white powder observed correspond to the matter detached from both surfaces.

Figure 46. Debris product of the abrasion after sliding PPE/PS+20%GF against itself

In the end, the wear generated in both surfaces for each combination is represented in *Figure* **47**. It can be abstracted than the best partners for PPE/PS+20%GF are POM, PA6.12+30%GF, PA66+MoS_2 and PBT+15%GF and, again, that sliding a thermoplastic against itself results in bad tribological properties.

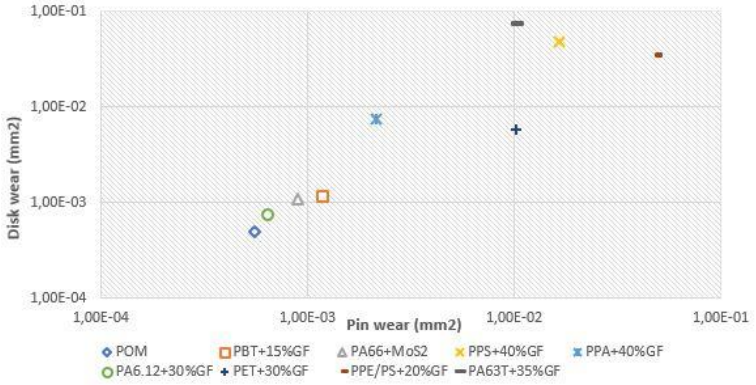

Figure 47. Wear rate caused for each combination to both pin and disk geometries for PPE/PS+20%GF based disks

Following the procedure, the combinations punctuated by their performance in friction and wear test are shown in *Figure* **48**.

	POM	PBT + 15%GF	PA66 + MoS_2	PPS + 40%GF	PPA + 40%GF	PA6.12 + 30%GF	PET + 30%GF	PPE/PS + 20%GF	PA6-3-T + 35%GF
Friction coefficient	1	8	2	6	3	3	5	9	7
Wear rate	1	4	3	7	5	2	6	9	8
Total	**2**	**12**	**5**	**13**	**8**	**5**	**11**	**18**	**15**

Figure 48. Sorted candidates from best (1) to worst (9) considering friction and wear displayed against PPE/PS+20%GF based disk

Apart from POM and PA66+MoS_2, the priority candidates to consider for working against PPE/PS+20%GF are the polyamides PA6.12+30%GF and PPA+40%GF.

8.4. COMBINATION'S CHOICE

The aim of the current project is to find the best combination of thermoplastics for our system constituted by the three studied pieces. To compare each polymeric pair performance fairly, a final score has been calculated for all of them, considering all the parameters tested before and during this project. As the ceramic holder's raw material is already fixed but the housing's not, each racord's candidate is punctuated twice, once considering PBT+15%GF as the housing's raw material and other considering PPE/PS+20%GF.

The final score (S_F) is calculated following *Eq.***9**, in which S_{NT} is the non-tribological score, given to each raw material depending on their performance in non-tribological tests, and S_T is the tribological score, the one obtained for each polymeric pair in the tribological test. Furthermore, it is considered the sum of parameters such as creep, mechanical resistance, dimensional stability associated to water absorption, thermal expansion and cost weights twice the tribological performance.

$$S_F = \frac{2}{3} \cdot S_{NT} + \frac{1}{3} \cdot S_T \tag{9}$$

Likewise, the non-tribological score is calculated following *Eq.***10**, in which S_{RACORD} is the punctuation given to each racord's candidate, shown in *Figure* **24**, and $S_{HOUNSING}$ is the punctuation given to PBT+15%GF or PPE/PS+20%GF in *Figure* **15**. The ponderations, like in the

other cases, are subjectively given considering the role each item has on the system. As mentioned through the project, racord is the most critical and limiting item and so it is reflected in the ponderation.

$$S_{NT} = \frac{3}{4} \cdot S_{RACORD} + \frac{1}{4} \cdot S_{HOUSING} \quad (10)$$

For the tribological score, it is considered that both the tribological behaviour between the racord and the ceramic holder and the tribological behaviour between the racord and the housing are equally important. It is calculated as of *Eq.***11**, in which $\alpha_{POM(candidate)}$ is the tribological performance score of each racord's candidate against POM and $\alpha_{X(candidate)}$ is the tribological performance score for each racord's candidate against the housing's candidates, being *x* = PBT+15%GF or PPE/PS+20%GF.

$$S_T = \frac{\alpha_{POM}(candidate) + \alpha_X(candidate)}{2} \quad (11)$$

Finally, the same importance is given to friction and wear, so the tribological performance score is calculated as the average of both. Likewise, wear is always considered as the average of the wear suffered by the pin and the disk.

To calculate the scores, the difference between the highest and the lowest reverses[8] of the values has been divided in ten intervals to give a score between 0 (to the worst candidate) to 10 (to the best).

[8] Both the friction coefficient and the wear rate are desired as low as possible

8.4.1. Scores considering a PBT+15%GF based housing

Using the equations given above, both tribological performances and the tribological score for each racord's candidate are given in *Table* **9**, *Table* **10** and *Table* **11**. Continuedly, the non-tribological score is presented in *Table* **12**.

Table 9. Tribological performance score against POM for each racord's candidate

Material	**POM**	**PBT+15%GF**	**PA66+MoS_2**	**PPS+40%GF**	**PPA+40%GF**
α_{POM}	0,0	Not candidate	9,3	2,9	6,5
Material	**PA6.12+30% GF**	**PET+30%GF**	**PPE/PS+20% GF**	**PA63T+35% GF**	
α_{POM}	5,1	4,4	5,0	4,7	

Table 10. Tribological performance score against PBT+15%GF for each racord's candidate

Material	**POM**	**PBT+15%GF**	**PA66+MoS_2**	**PPS+40%GF**	**PPA+40%GF**
$\alpha_{PBT+15\%GF}$	2,1	Not candidate	2,0	2,4	8,7
Material	**PA6.12+30% GF**	**PET+30%GF**	**PPE/PS+20% GF**	**PA63T+35% GF**	
$\alpha_{PBT+15\%GF}$	2,2	5,3	2,8	9,6	

Table 11. Tribological score considering a PBT+15%GF based housing for each racord's candidate

Material	**POM**	**PBT+15%GF**	**PA66+MoS_2**	**PPS+40%GF**	**PPA+40%GF**
S_T	1,0	Not candidate	5,7	2,6	7,6
Material	**PA6.12+30% GF**	**PET+30%GF**	**PPE/PS+20% GF**	**PA63T+35% GF**	
S_T	3,6	4,9	3,9	7,2	

Thus, in terms of tribology for the system POM – candidate – PBT+15%GF, polyphthalamides' family highlight over the other candidates.

Table 12. Non-tribological score for each racord's candidate considering a PBT+15%GF based housing

Material	**POM**	**PBT+15%GF**	**PA66+MoS_2**	**PPS+40%GF**	**PPA+40%GF**
S_{NT}	6,2	Not candidate	6,1	7,6	7,2
Material	**PA6.12+30% GF**	**PET+30%GF**	**PPE/PS+20% GF**	**PA63T+35% GF**	
S_{NT}	6,9	7,5	7,7	(5,9)[9]	

Theoretically, adding glass fibres to PA6-3-T the torque resistance, dimensional stability and thermal expansion should enhance. Even the price would decrease as the polymeric base's cost is rather high. Hence, considering the scores obtained by PA6-3-T based racord, the calculated non-tribological score is conservative, but surely not overestimated.

The final scores, considering tribological and non-tribological parameters for the combination POM – candidate – PBT+15%GF are given in *Table* **13**.

Table 13. Final score for each racord's candidate considering POM and PBT+15%GF as the raw materials for the ceramic holder and the housing, respectively

Material	**POM**	**PBT+15%GF**	**PA66+MoS_2**	**PPS+40%GF**	**PPA+40%GF**
S_{NT}	4,5	Not candidate	6,0	6,0	7,3
Material	**PA6.12+30% GF**	**PET+30% GF**	**PPE/PS+20% GF**	**PA63T+35% GF**	
S_{NT}	5,8	6,6	6,4	(6,3)[10]	

[9] Although PA6-3-T+35%GF racords could not be injected, a lower estimation can be done with the values of PA6-3-T based racords

[10] The real score can be forecasted higher

8.4.2. Scores considering a PPE/PS+20%GF based housing

The punctuation process is now repeat considering the POM – candidate – PPE/PS+20%GF as the raw materials for ceramic holder – racord – housing system. The tribological performance score against POM is already shown in *Table* **9** for each racord's candidate. Tribological performance score against PPE/PS+20%GF and the pertinent tribological score are shown in *Table* **14** and *Table* **15**.

Table 14. Tribological performance score against PPE/PS+20%GF for each racord's candidate

Material	**POM**	**PBT+15%GF**	**PA66+MoS_2**	**PPS+40%GF**	**PPA+40%GF**
S_{NT}	3,2	Not candidate	1,5	0,1	0,8
Material	**PA6.12+30% GF**	**PET+30% GF**	**PPE/PS+20% GF**	**PA63T+35% GF**	
S_{NT}	1,3	0,4	0,0	0,1	

Table 15. Tribological score considering a PPE/PS+20%GF based housing for each racord's candidate

Material	**POM**	**PBT+15%GF**	**PA66+MoS_2**	**PPS+40%GF**	**PPA+40%GF**
S_{NT}	1,6	Not candidate	5,4	1,5	3,7
Material	**PA6.12+30% GF**	**PET+30% GF**	**PPE/PS+20% GF**	**PA63T+35% GF**	
S_{NT}	3,2	2,4	2,5	2,4	

The tribological scores supposing PPE/PS+20%GF based housings are low because of the bad tribological behaviour shown during the tests.

In *Table* **16** are shown the non-tribological scores for each racord's candidate, considering now PPE/PS+20%GF as the housing's raw material.

Lastly, *Table* **17** shows the final scores calculated considering both the tribological and non-tribological punctuations for the combination POM – candidate – PPE/PS+20%GF.

Table 16. Non-tribological score for each racord's candidate considering a PPE/PS+20%GF based housing

Material	**POM**	**PBT+15%GF**	**PA66+MoS_2**	**PPS+40%GF**	**PPA+40%GF**
S_{NT}	6,7	Not candidate	6,6	8,1	7,7
Material	**PA6.12+30% GF**	**PET+30%GF**	**PPE/PS+20% GF**	**PA63T+35% GF**	
S_{NT}	7,4	8,0	8,2	(6,4)[11]	

Table 17. Final score for each racord's candidate considering POM and PPE/PS+20%GF as the raw materials for the ceramic holder and the housing, respectively

Material	**POM**	**PBT+15%GF**	**PA66+MoS_2**	**PPS+40%GF**	**PPA+40%GF**
S_{NT}	5	Not candidate	6,2	5,9	6,4
Material	**PA6.12+30% GF**	**PET+30% GF**	**PPE/PS+20% GF**	**PA63T+35% GF**	
S_{NT}	6,0	6,1	6,3	(5,1)[12]	

[11] Again, calculated with the values of PA6-3-T based racords
[12] The real score can be forecasted higher

9. CONCLUSIONS

The aim of the current project was to find out the thermoplastic combination with the best tribological properties to use in the system housing – racord – ceramic holder. After the fulfilment of the objectives and analysing the results, the obtained conclusions are the following:

- After studying the availably, mechanical properties, dimensional stability associated to moisture absorption, thermal expansion, processability and cost, the selection process conducted before tribological tests has determined POM, PBT+15%GF, PA66+MoS_2, PPS+40%GF, PPA+40%GF, PA6.12+30%GF, PET+30%GF, PPE/PS+20%GF and PA63T+35%GF are the potential candidates to use in the stated application.
- It has been demonstrated that using a self-mated combination in sliding systems leads to a higher friction coefficient and wear rate.
- Considering both tribological and non-tribological performances, the resulting best combination is PBT+15%GF (housing) – PPA+40%GF (racord) – POM (ceramic holder), followed by PBT+15%GF – PET+30%GF – POM combination.
- The use of PPE/PS+20%GF as the housing's raw material is justified for when enhance creep resistance becomes a critical limitation. To this end, the combination PPE/PS+20%GF – PPA+40%GF – POM is the best option with the third highest score among the tested combinations.

Future work should carry out optimal trials with PA6-3-T+35%GF based racords, since even being underestimated its combination with PBT+15%GF and POM still holds the fifth highest score.

10. REFERENCES AND NOTES

[1] G. Wypych, “POM polyoxymethylene,” *Handb. Polym.*, pp. 473–478, 2012.

[2] Y. J. Mergler, R. P. Schaake, and A. J. Huis in’t Veld, “Material transfer of POM in sliding contact,” *Wear*, vol. 256, no. 3–4, pp. 294–301, 2004.

[3] Z. Rymuza, “Tribology of polymers,” *Arch. Civ. Mech. Eng.*, vol. 7, no. 4, pp. 177–184, 2007.

[4] A. Pogačnik and M. Kalin, “Parameters influencing the running-in and long-term tribological behaviour of polyamide (PA) against polyacetal (POM) and steel,” *Wear*, vol. 290–291, pp. 140–148, 2012.

[5] L. Wojciechowski and T. G. Mathia, “Focus on the concept of pressure-velocity-time (pVt) limits for boundary lubricated scuffing,” *Wear*, vol. 402–403, no. February, pp. 179–186, 2018.

[6] M. S. Mohammadi, M. Ghani, M. Komeili, B. Crawford, and A. S. Milani, “The effect of manufacturing parameters on the surface roughness of glass fibre reinforced polymer moulds,” 2017.

[7] Y. Xu, Q. Wu, Y. Lei, and F. Yao, “Creep behavior of bagasse fiber reinforced polymer composites,” *Bioresour. Technol.*, vol. 101, no. 9, pp. 3280–3286, 2010.

[8] “Maxwell and Kelvin Elements.” [Online]. Available: http://polymerdatabase.com/polymer physics/Maxwell-Kelvin.html. [Accessed: 24-May-2018].

[9] C. Martins, V. Pinto, R. M. Guedes, and A. T. Marques, “Creep and Stress Relaxation Behaviour of PLA-PCL Fibres - A Linear Modelling Approach,” *Procedia Eng.*, vol. 114, pp. 768–775, 2015.

[10] K. A. Harries, Q. Guo, and D. Cardoso, “Creep and creep buckling of pultruded glass-

reinforced polymer members," *Compos. Struct.*, vol. 181, pp. 315–324, 2017.

[11] "EN817.pdf." .

[12] G. Baschek, G. Hartwig, and F. Zahradnik, "Effect of water absorption in polymers at low and high temperatures," *Polymer (Guildf).*, vol. 40, no. 12, pp. 3433–3441, 1999.

[13] Bada, "Absorción de agua en poliamidas," pp. 5–6.

[14] "ASTM G99 - 04a Standard Test Method for Wear Testing with a Pin-on-Disk Apparatus." [Online]. Available: https://www.astm.org/DATABASE.CART/HISTORICAL/G99-04A.htm. [Accessed: 31-May-2018].

[15] M. M. Farag, *Materials and process selection in engineering design*. 2014.

APPENDICES

APPENDIX 1. FORMULATIONS OF THE CANDIDATES

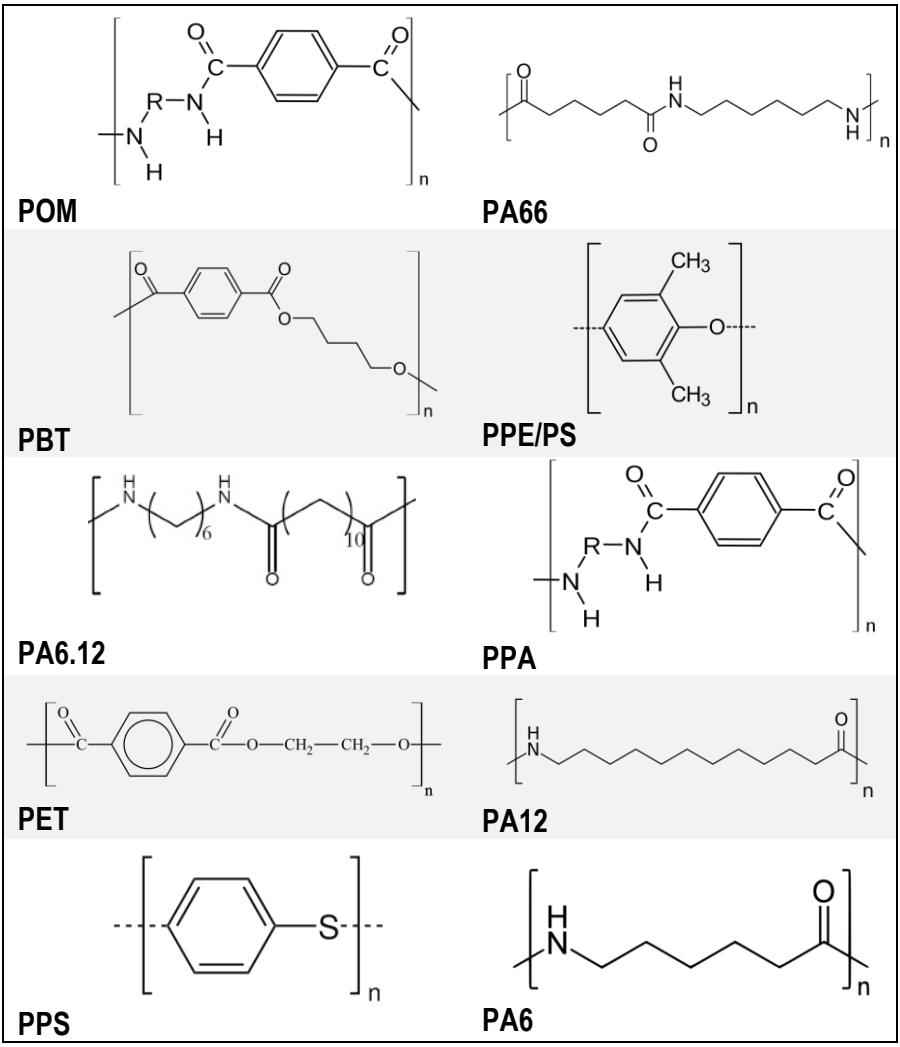

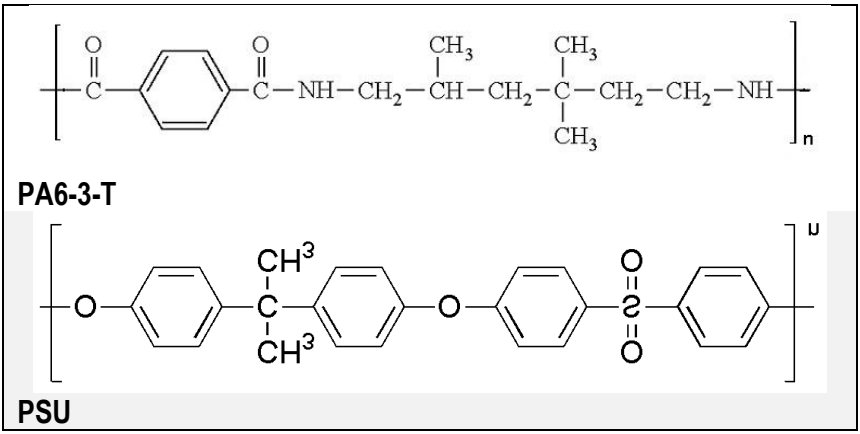

Images from Wikimedia Commons

APPENDIX 2. SAUNA CONDITIONS SIMULATION TEST

Objective: The test was done to compare the dimensional stability associated to moisture absorption of POM and PA66+MoS2. It has been conducted using a controlled atmosphere chamber, seen in *Figure* **49**.

Conditions:

- The test was done to racords injected with the studied raw materials.
- Two samples of each raw material were tested.
- Sauna conditions: 40ºC and 100% relative humidity (H_r).
- The samples remained in the sauna tank for a week.
- Two measures were taken to evaluate the dimensional increase, one transversal to the injection point and the other longitudinal to the injection point. The variation plotted in *Figure* **1** is the average of both.
- Before measuring, the racords were submerged in water at room temperature to remove dilatation factor and dried with air to remove the adsorbed water on the surface.

Figure 49. "Sauna" tank

APPENDIX 3. ENDURA SN-35 S/D EVO1 DRAWING

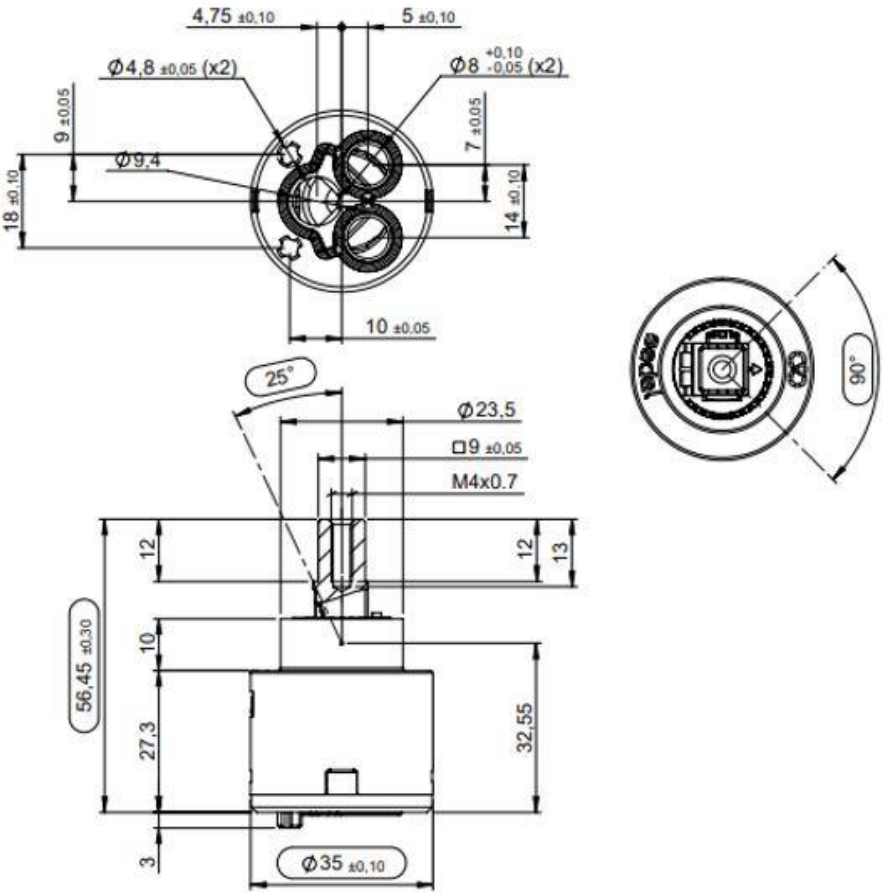

APPENDIX 4. TRIBOLOGY AGAINST POM

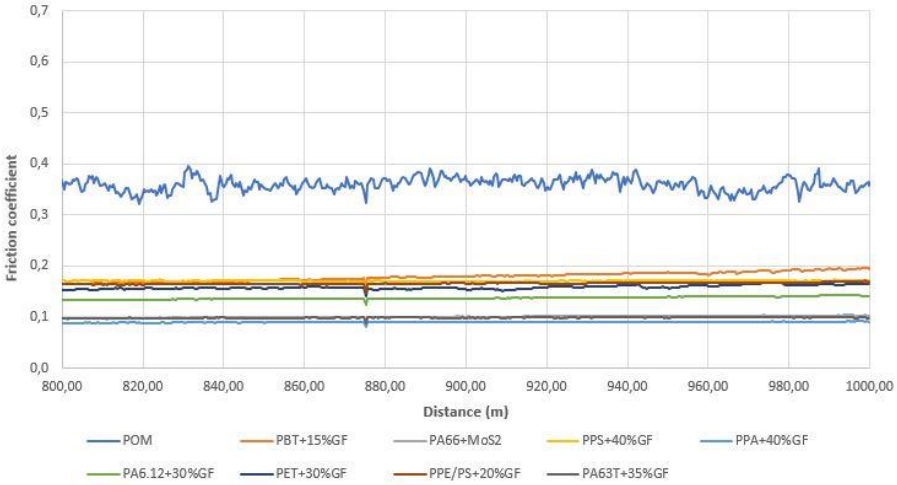

Figure 50. Evolution of the candidates' friction coefficient in function of the distance covered when sliding against POM in last 200 m

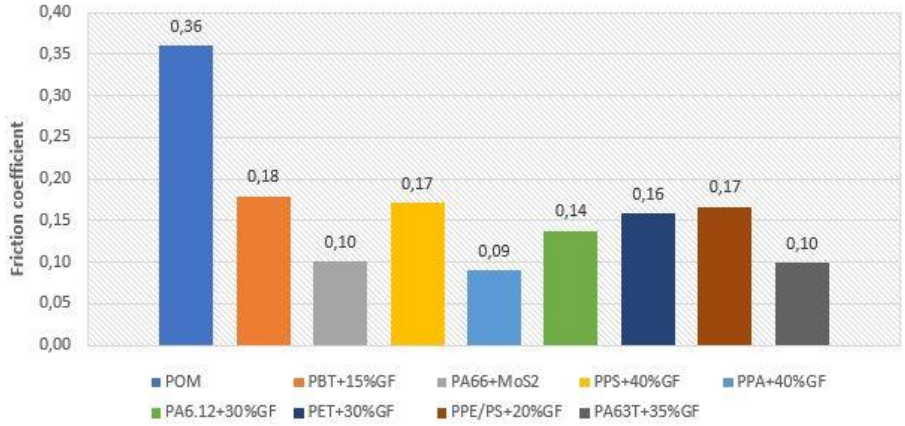

Figure 51. Representation of the friction coefficients measured for the candidates against POM

APPENDIX 5. TRIBOLOGY AGAINST PBT+15%GF

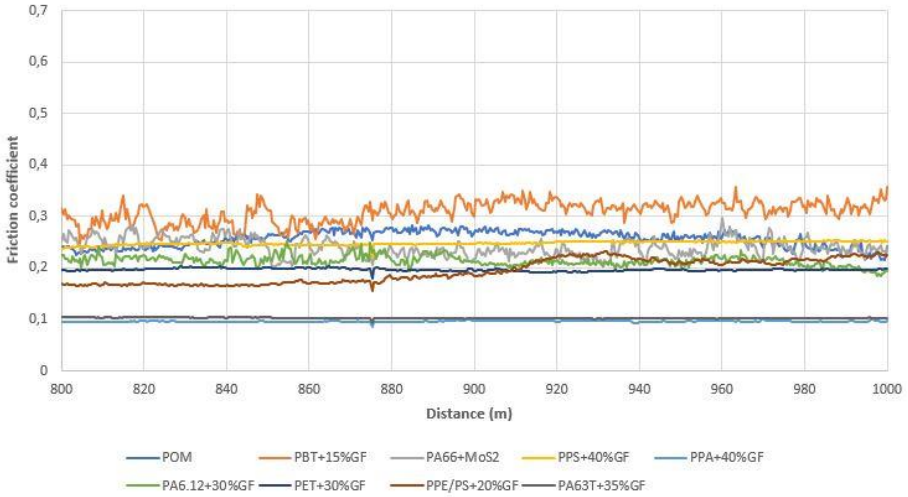

Figure 52. Evolution of the candidates' friction coefficient in function of the distance covered when sliding against PBT+15%GF in last 200 m

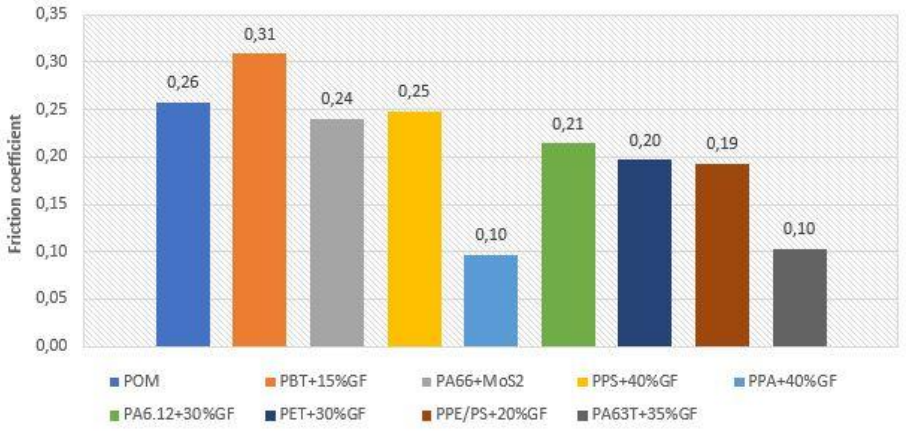

Figure 53. Representation of the friction coefficients measured for the candidates against PBT+15%GF

APPENDIX 6. TRIBOLOGY AGAINST PPE/PS+20%GF

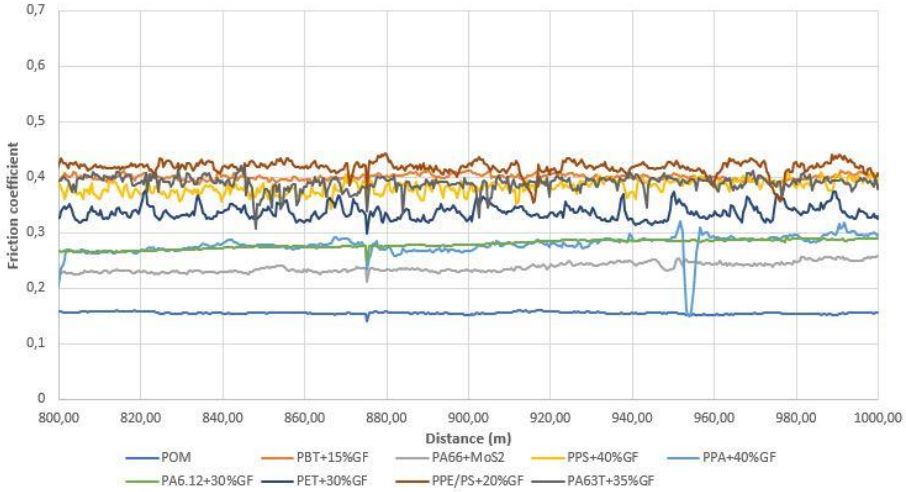

Figure 54. Evolution of the candidates' friction coefficient in function of the distance covered when sliding against PPE/PS+20%GF in last 200 m

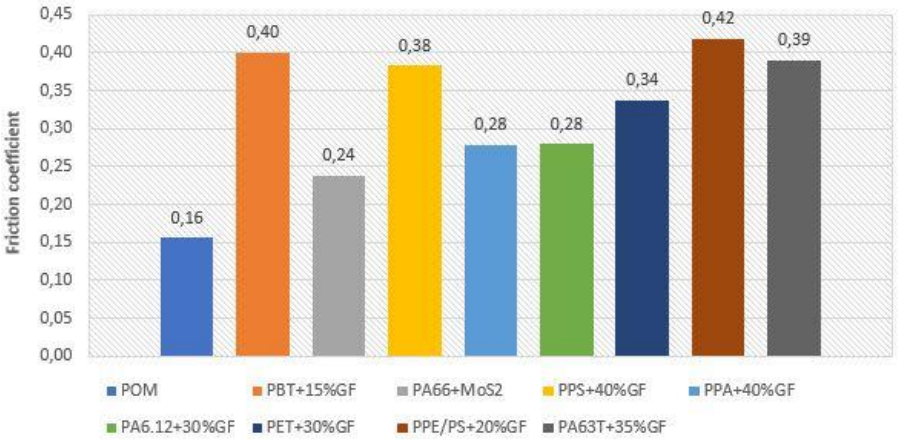

Figure 55. Representation of the friction coefficients measured for the candidates against PPE/PS+20%GF

APPENDIX 7. FIGURES LIST

*Figure 1. Dimensional increase and water absorption for PA66+MoS_2 and POM under sauna conditions simulation test (**67**)* *10*
Figure 2. Assembled ENDURA SN-35 S/D - EVO1 cartridge 3D *12*
Figure 3. Components of an ENDURA SN-35 S/D - EVO1 cartridge *13*
Figure 4. Top view of the ceramic discs (a) Fixed ceramic. (b) Mobile ceramic. *14*
Figure 5. Lever at none aperture angle position (a) Profile view. (b) Plan view *14*
Figure 6. Lever at maximum aperture angle position (a) Profile view. (b) Plan view *15*
Figure 7. Varying the superimposition of the inlets and outlet from left (totally hot water) to right (totally cold water) *15*
Figure 8. From left to right: housing, racord and ceramic holder *17*
Figure 9. Isometric and plan views of the studied components. In red, those contact zones sensitive to friction and wear *18*
Figure 10. Burgers model (four element model) [9] *19*
Figure 11. General description of material creep behaviour [10] *20*
Figure 12. Device used to measure the compressive force generated when the torque is applied *21*
Figure 13. Representation of the compressive force according to the torque applied *22*
Figure 14. Trade-off between material indexes M_1 and M_2 for the candidates *23*
Figure 15. Housing's raw material selection matrix *24*
Figure 16. Representation of an assembled lever-pin-racord system *24*
Figure 17. Representation of the force applied to the stoppers and their functional section *25*
Figure 18. FEA simulations in terms of (a) von Mises' stress (b) deformation and (c) factor of safety *26*
Figure 19. Relation between the inverses of E and σe for the selected candidates *27*

Figure 20. Relation between the inverse of the product of E and σe and the price for the selected candidates *28*
Figure 21. Torque resistance test procedure *30*
Figure 22. Percentage of water absorption measured for each raw material after two, four and six hours submerged *31*
Figure 23. Dimensional increase for each raw material after two, four and six hours submerged *31*
Figure 24. Decision matrix showing the score of each material for their performance in each test. Every parameter has an associated subjective ponderation based on experience. According to the score, a final decision is taken. *33*
Figure 25. Assembled ceramic holder and mobile ceramic *34*
Figure 26. Representation of all the combinations tested with the tribometer device *35*
Figure 27. Ball-on-disk device *36*
Figure 28. Original mechanism of the ball-on-disk device *36*
Figure 29. Isometric view of the pin and the disk designs compared to an ENDURA SN-35 S/D - EVO1 cartridge's ceramic holder *37*
Figure 30. Isometric view of (a) the joining item & (b) a disk fixed to the joining item *38*
Figure 31. Primary components of a mould, (a) the injection mould and (b) the ejector mould *38*
Figure 32. Mechanized joining item and pins and disks made of (from top left to bottom right) PET+30%GF, PA66+MoS2, PA6.12+30%GF, PA6-3-T+35%GF , PPA+40%GF, PPE/PS+20%GF, PPS+40%GF, PBT+15%GF and POM *39*
Figure 33. Modified device once set the component *39*
*Figure 34. Evolution of the candidates' friction coefficient in function of the distance covered when sliding against POM (**71**)* *43*
Figure 35. Representation of the processes involved in adhesive wear [15] *44*
Figure 36. Wear rate caused by the candidates on POM based disk *45*
Figure 37. Wear rate caused for each combination to both pin and disk geometries for POM based disks *46*
Figure 38. Sorted candidates from best (1) to worst (9) considering friction and wear displayed against POM based disk *46*

*Figure 39. Evolution of the candidates' friction coefficient in function of the distance covered when sliding against PBT+15%GF (**73**)* *47*
Figure 40. Wear rate caused by the candidates on PBT+15%GF based disk *47*
Figure 41. Wear rate caused for each combination to both pin and disk geometries for PBT+15%GF based disks *48*
Figure 42. Sorted candidates from best (1) to worst (9) considering friction and wear displayed against PBT+15%GF based disk *48*
*Figure 43. Evolution of the candidates' friction coefficient in function of the distance covered when sliding against PPE/PS+20%GF (**75**)* *49*
Figure 44. Wear rate caused by the candidates on PPE/PS+20%GF based disk *50*
Figure 45. Amplified representation of wear rate caused by the candidates on PPE/PS+20%GF based disk *50*
Figure 46. Debris product of the abrasion after sliding PPE/PS+20%GF against itself *51*
Figure 47. Wear rate caused for each combination to both pin and disk geometries for PPE/PS+20%GF based disks *51*
Figure 48. Sorted candidates from best (1) to worst (9) considering friction and wear displayed against PPE/PS+20%GF based disk *52*
Figure 49. "Sauna" tank *67*
Figure 50. Evolution of the candidates' friction coefficient in function of the distance covered when sliding against POM in last 200 m *71*
Figure 51. Representation of the friction coefficients measured for the candidates against POM *71*
Figure 52. Evolution of the candidates' friction coefficient in function of the distance covered when sliding against PBT+15%GF in last 200 m *73*
Figure 53. Representation of the friction coefficients measured for the candidates against PBT+15%GF *73*
Figure 54. Evolution of the candidates' friction coefficient in function of the distance covered when sliding against PPE/PS+20%GF in last 200 m *75*
Figure 55. Representation of the friction coefficients measured for the candidates against PPS/PS+20%GF *75*

APPENDIX 8. TABLES LIST

Table 1. Base materials for the thermoplastic components in an ENDURA SN-35 S/D - EVO1 cartridge 12
Table 2. Contour conditions for a housing 19
Table 3. Torque loss test results 21
Table 4. Raw materials injected and tested 29
Table 5. Thermal expansion coefficient measured for each candidate 32
Table 6. Friction coefficient for each candidate against POM 44
*Table 7. Friction coefficient for each candidate against PBT+15%GF (**73**)* 46
*Table 8. Friction coefficient for each candidate against PPE/PS+20%GF (**75**)* 49
Table 9. Tribological performance score against POM for each racord's candidate 54
Table 10. Tribological performance score against PBT+15%GF for each racord's candidate ... 54
Table 11. Tribological score considering a PBT+15%GF based housing for each racord's candidate 54
Table 12. Non-tribological score for each racord's candidate considering a PBT+15%GF based housing 55
Table 13. Final score for each racord's candidate considering POM and PBT+15%GF as the raw materials for the ceramic holder and the housing, respectively 55
Table 14. Tribological performance score against PPE/PS+20%GF for each racord's candidate 56
Table 15. Tribological score considering a PPE/PS+20%GF based housing for each racord's candidate 56
Table 16. Non-tribological score for each racord's candidate considering a PPE/PS+20%GF based housing 57
Table 17. Final score for each racord's candidate considering POM and PBT+15%GF as the raw materials for the ceramic holder and the housing, respectively 57